

ALMAを用いた太陽彩層構造と起 源研究について

末松芳法 (国立天文台)

ALMA太陽観測ワークショップ@京都
2012年10月3日

ALMA Obs the Sun

Wavelengths

Band 3: 84-116 GHz* (λ 3.6-2.6 mm)

Band 4: 125-163 GHz*

Band 6: 211-275 GHz*

Band 7: 274-373 GHz*

Band 8: 385-500 GHz*

Band 9: 602-720 GHz

Band10: 787-950 GHz (λ 0.4-0.3 mm)

Those are **thermal continua in quiet sun** (Intensity =Temperature).

(linear polarization is observed in all bands and circular in band7)

Spatial resolution (FOV) for the Sun (max baseline 2 km)

0.38" (62") at 100 GHz,

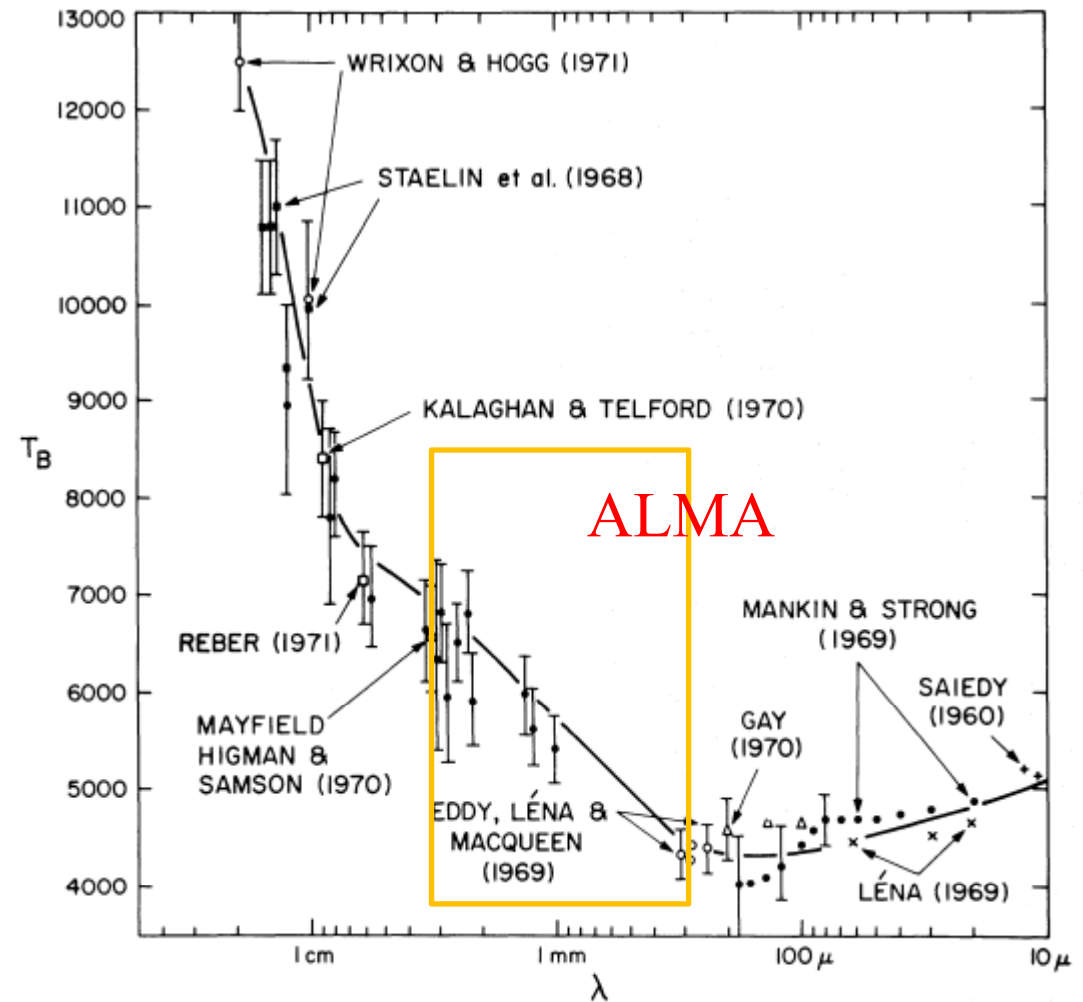
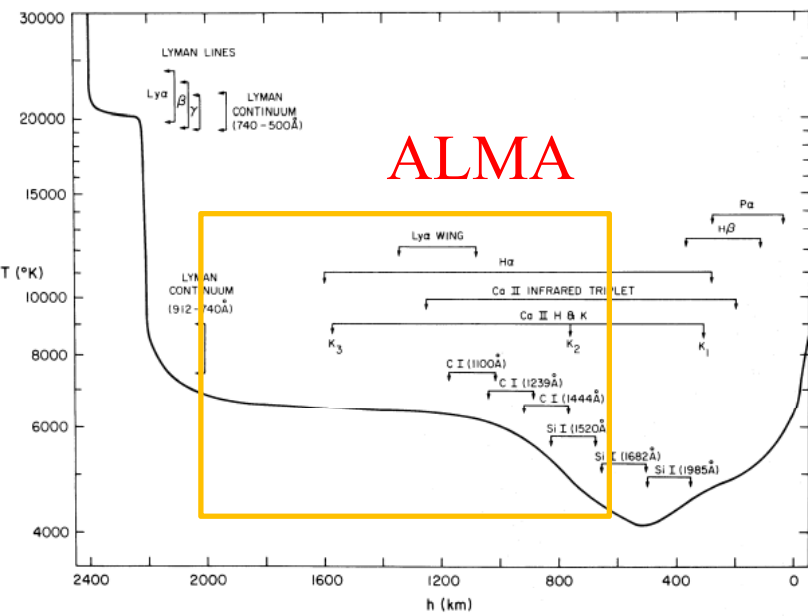
0.126" (18") at 300 GHz,

0.04" (7") at 950 GHz

Expected time cadence: 1 min

ALMA Observations of Quiet Sun

ALMA observes T-min –
chromosphere in high spatial
resolution (0.04"-0.4")



Vernazza et al. (1973) ApJ 184

ALMA Observations of Quiet Sun

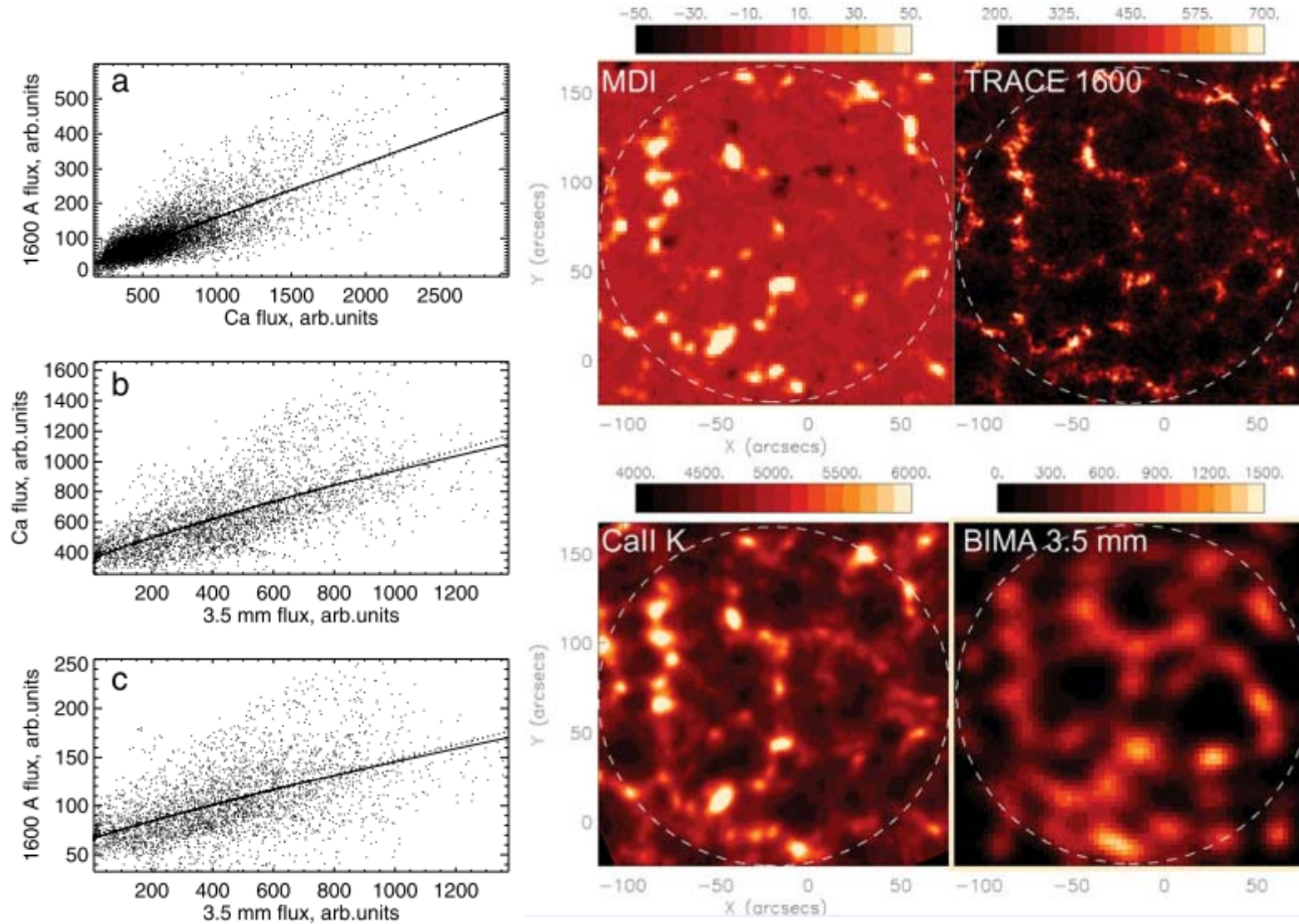
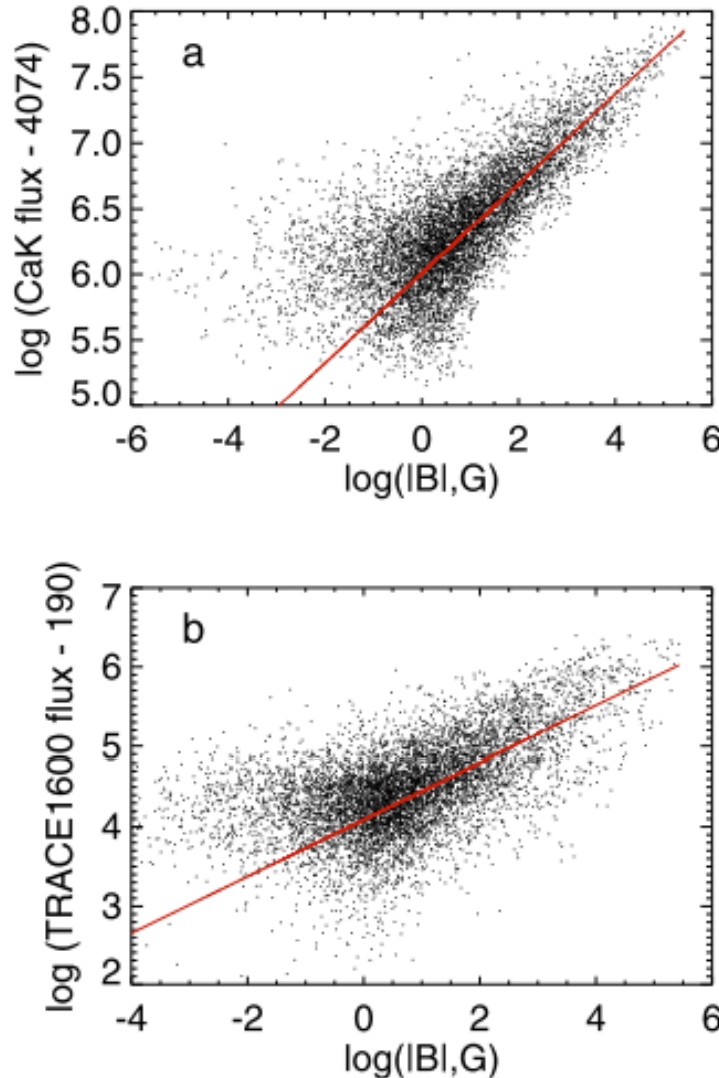


Figure 1. The solar chromosphere at 4 different wavelengths on May 18, 2004. From top left to bottom right: MDI longitudinal photospheric magnetogram, TRACE 1600 Å image, CaII K-line center image from BBSO and BIMA image at 3.5 mm. The images are created by averaging over 3.5h observational run. Dashed circles mark the 96 arcsec BIMA FOV containing flux. X and Y axes are in arcsec from the disk center.

Loukitcheva et al. (2009) A&A 497
 Loukitcheva et al. (2009) IAUS259

ALMA Observations of Quiet Sun

Loukitcheva et al. (2009) A&A 497



Log-log scatter plots for a) the Ca ii K-line excess mean intensity (after the subtraction of the zero flux) and b) TRACE 1600 Å excess mean intensity vs. the absolute value of the magnetic flux density (for 2 arcsec pixel size). The solid lines represent the least-squares power-law fits to the data.

高分解能観測の必要性

彩層：磁場が支配している

現象の高分解能像は重要（エネルギーの発生、流れがsmall-scaleで起こっている）

→ 起源（エネルギー解放の現場、機構）

→

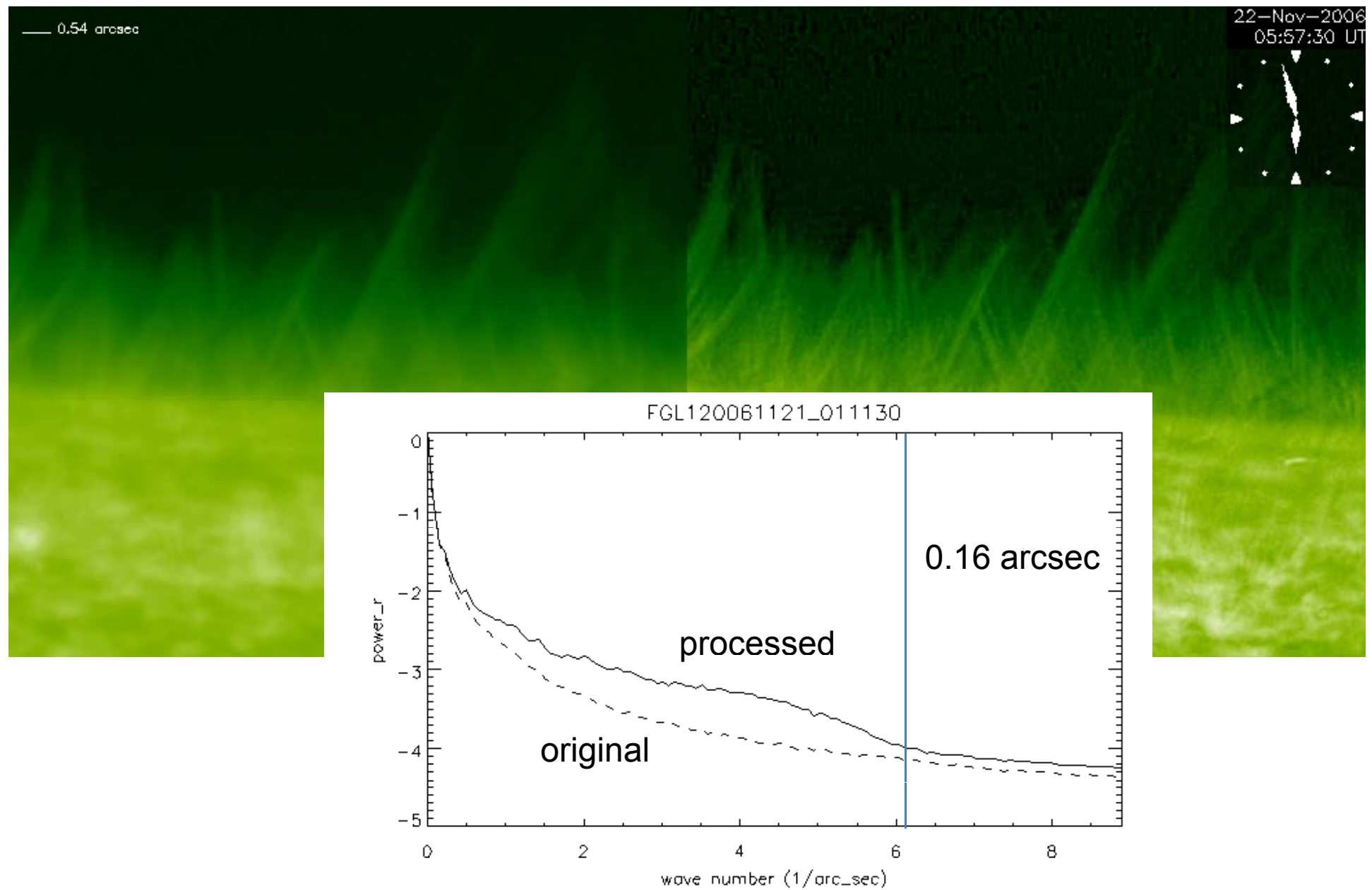
波動伝播、

質量、エネルギー輸送のソース



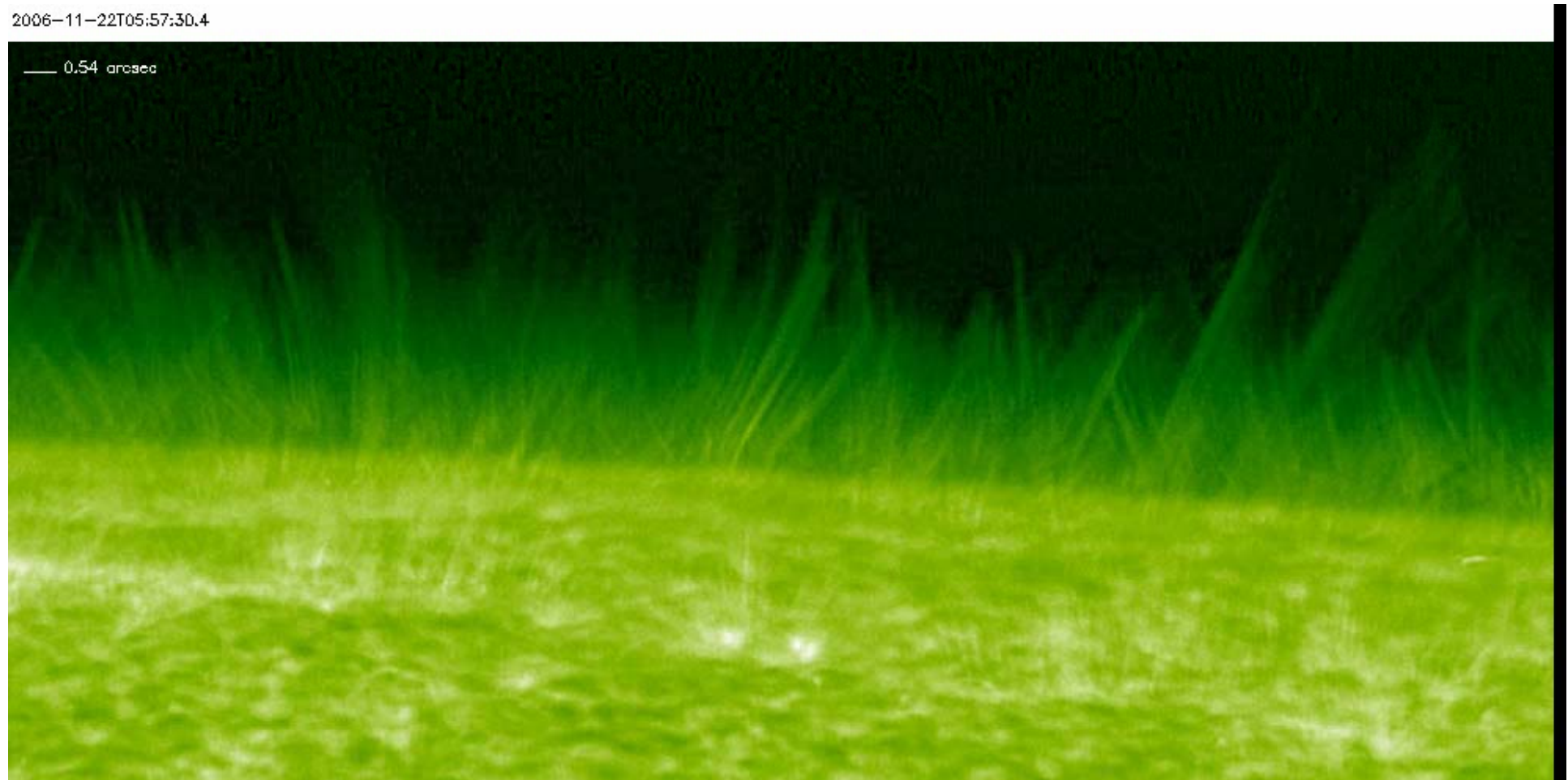
ALMAの彩層低部の高分解能、温度観測に期待

Power spectrum of processed Ca II H image



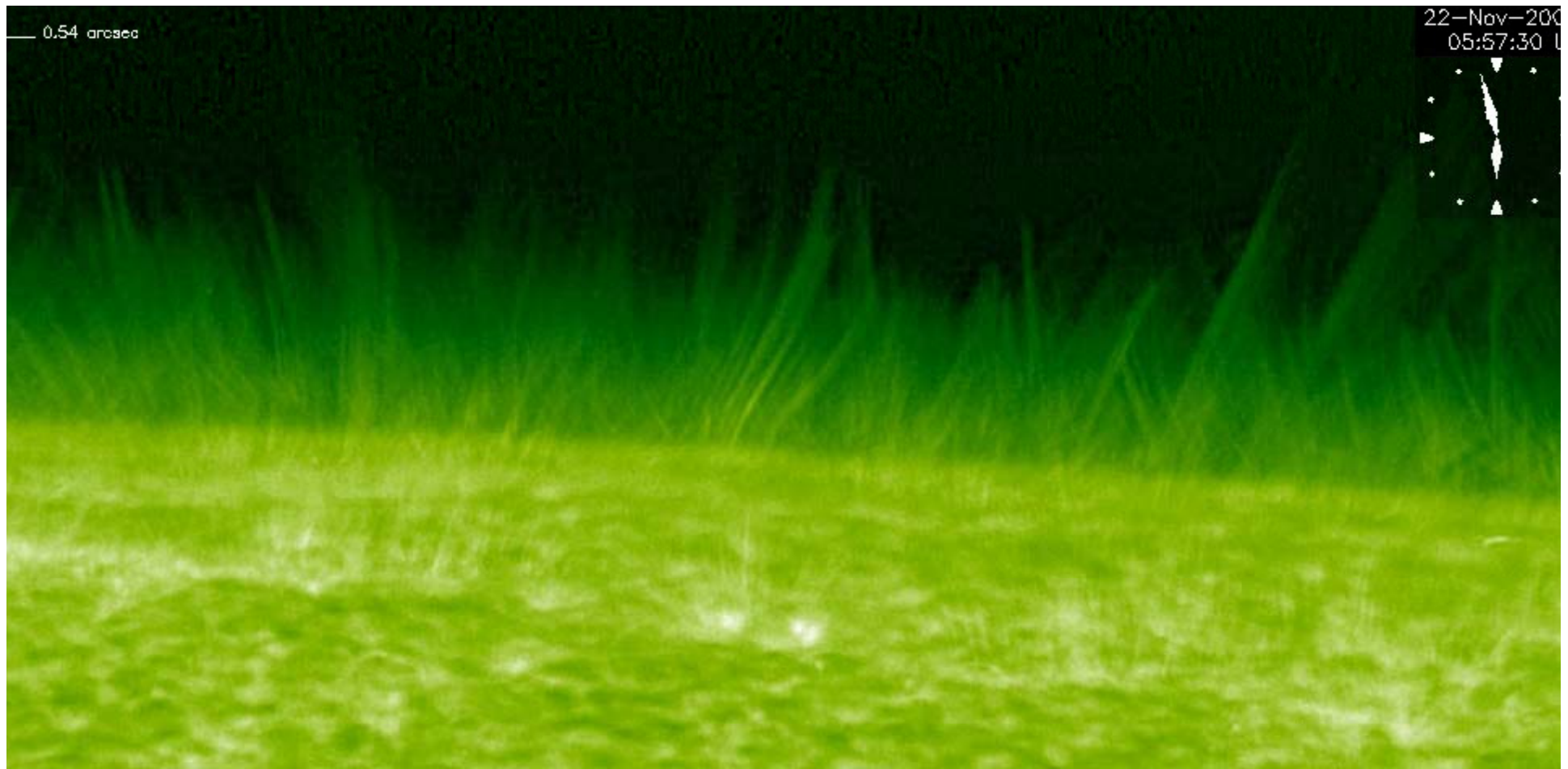
Fine-scale Limb structure of the chromosphere

Super-resolution ($\sim 0.1''$) reveals substructure of chromosphere (limb spicules)

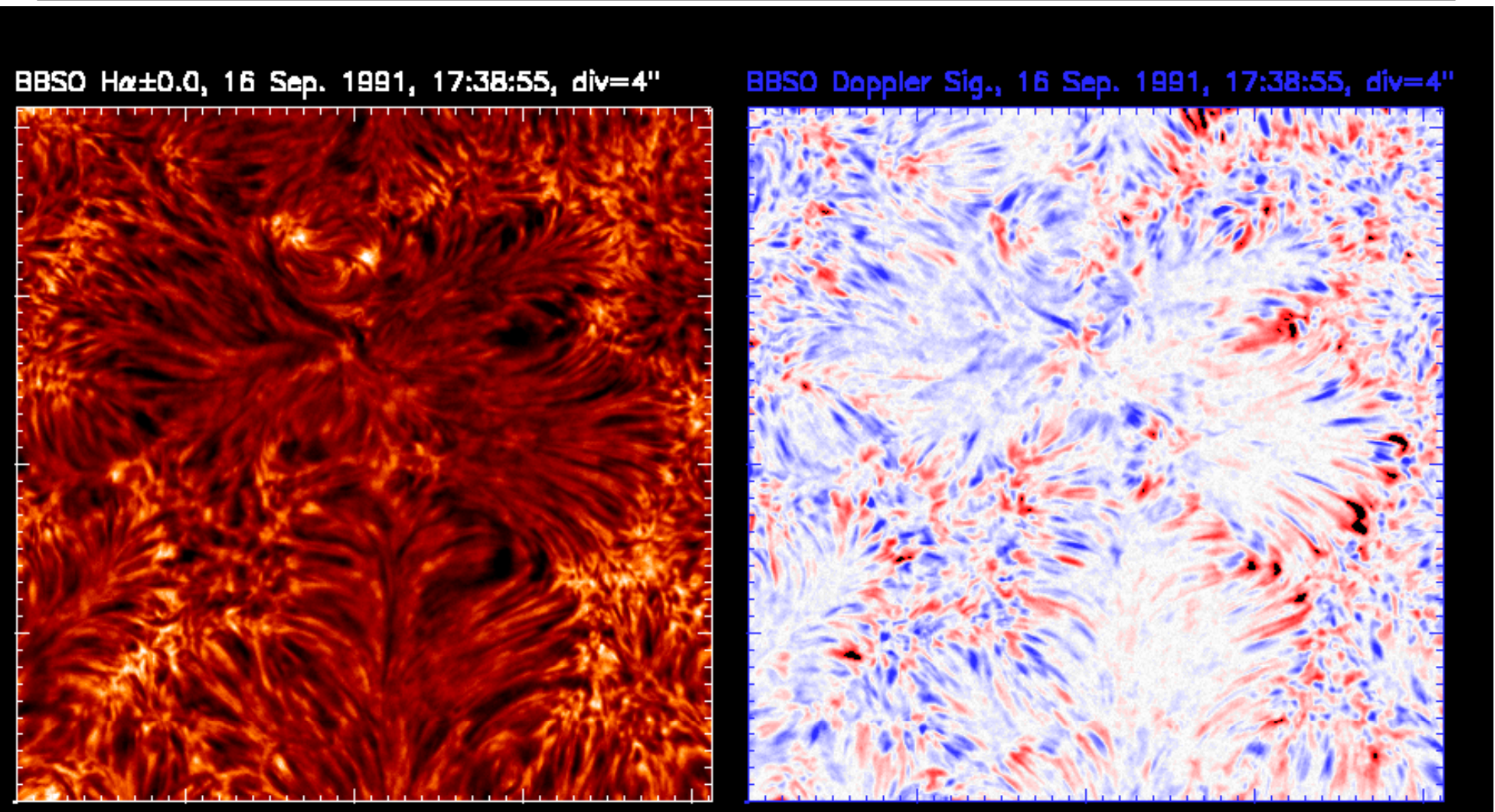


West limb: 22 Nov. 2006

Super-resolution ($\sim 0.1''$) reveals substructure of spicules

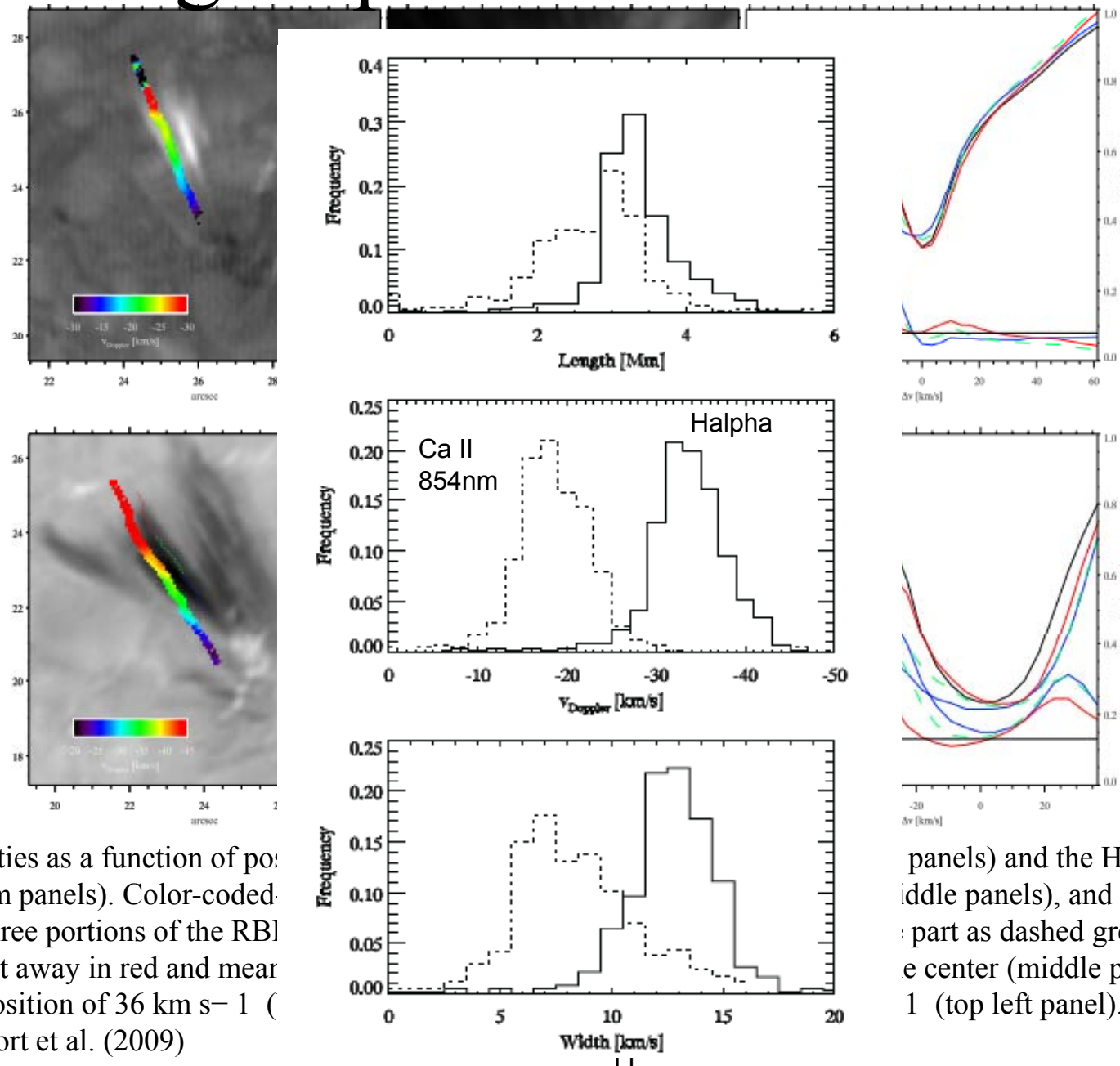


Chromospheric Structure and Motion



Hα line center image (left) and Dopplergram from $\text{H}\alpha \pm 0.65\text{\AA}$ (right). Blue structure indicates up-flow and red indicates downward motion. Doppler velocity is in the range $\sim 5\text{ km/sec}$ - 10 km/sec

Finding Rapid Blue-shift Excursion

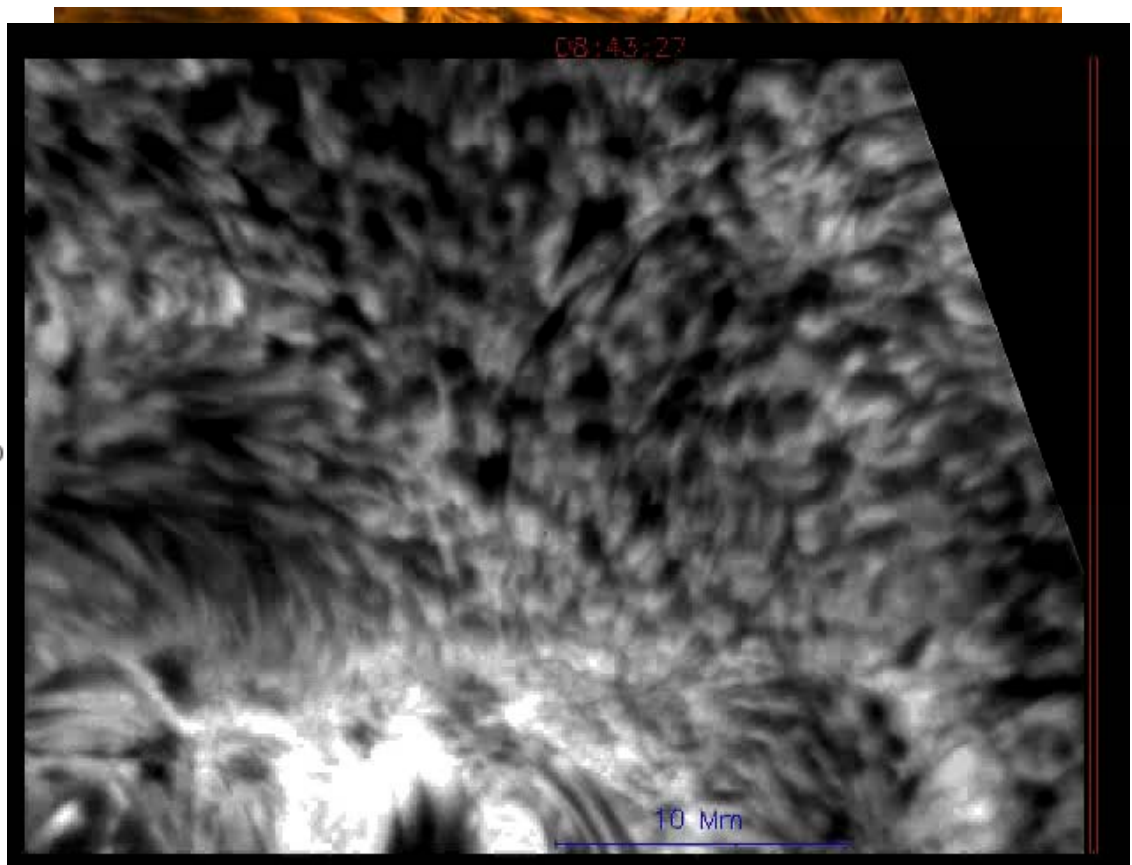
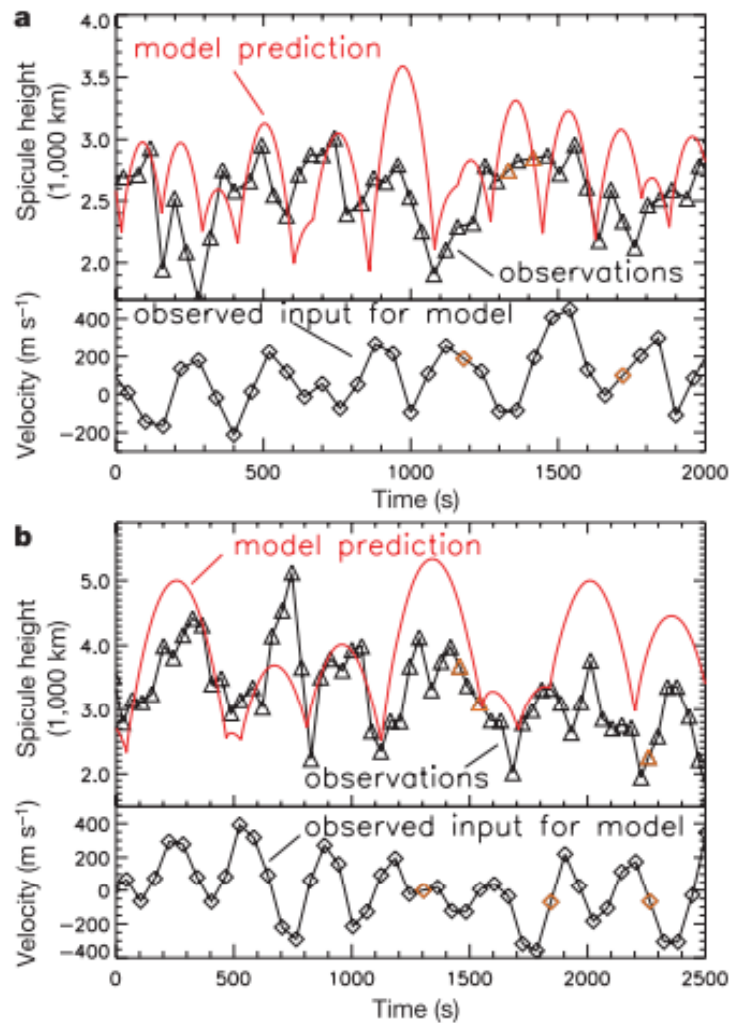


Properties as a function of position (bottom panels). Color-coded over three portions of the RB furthest away in red and nearest in blue position of 36 km s^{-1} (Roupe van der Voort et al. (2009))

panels) and the H α data set (middle panels), and mean spectra part as dashed green, part e center (middle panels), at a 1 (top left panel). Rouppe van

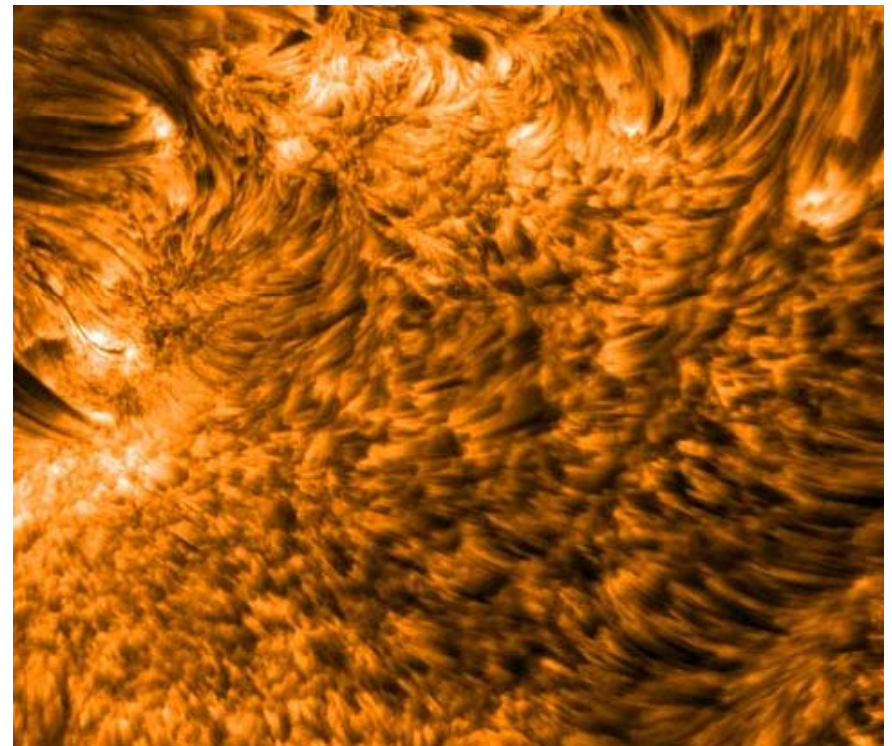
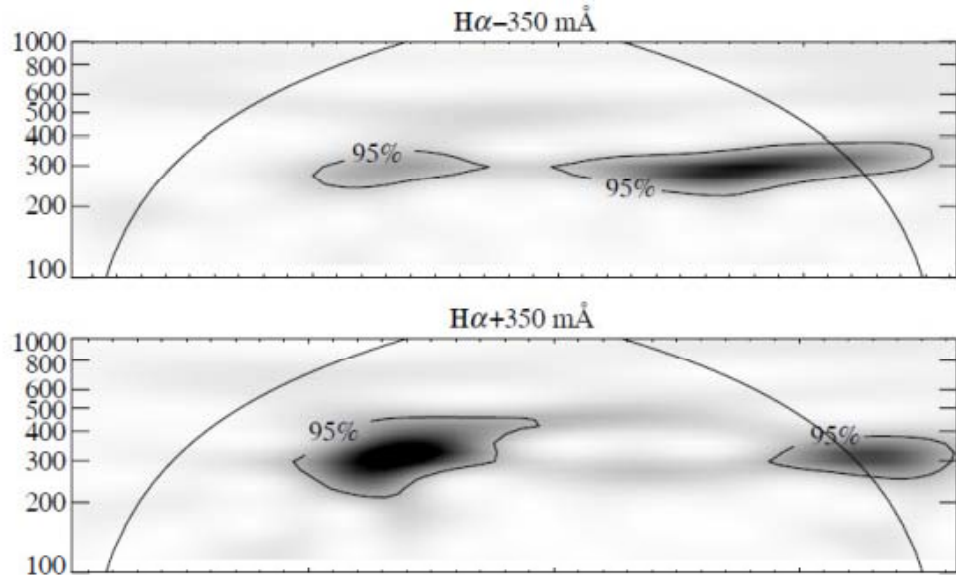
5分振動の漏れ出しによる彩層運動

De Pontieu et al. (2003, 2004) found that short spicules in plage region show 5-min recurrence and can be explained with photospheric 5-min oscillation driver.



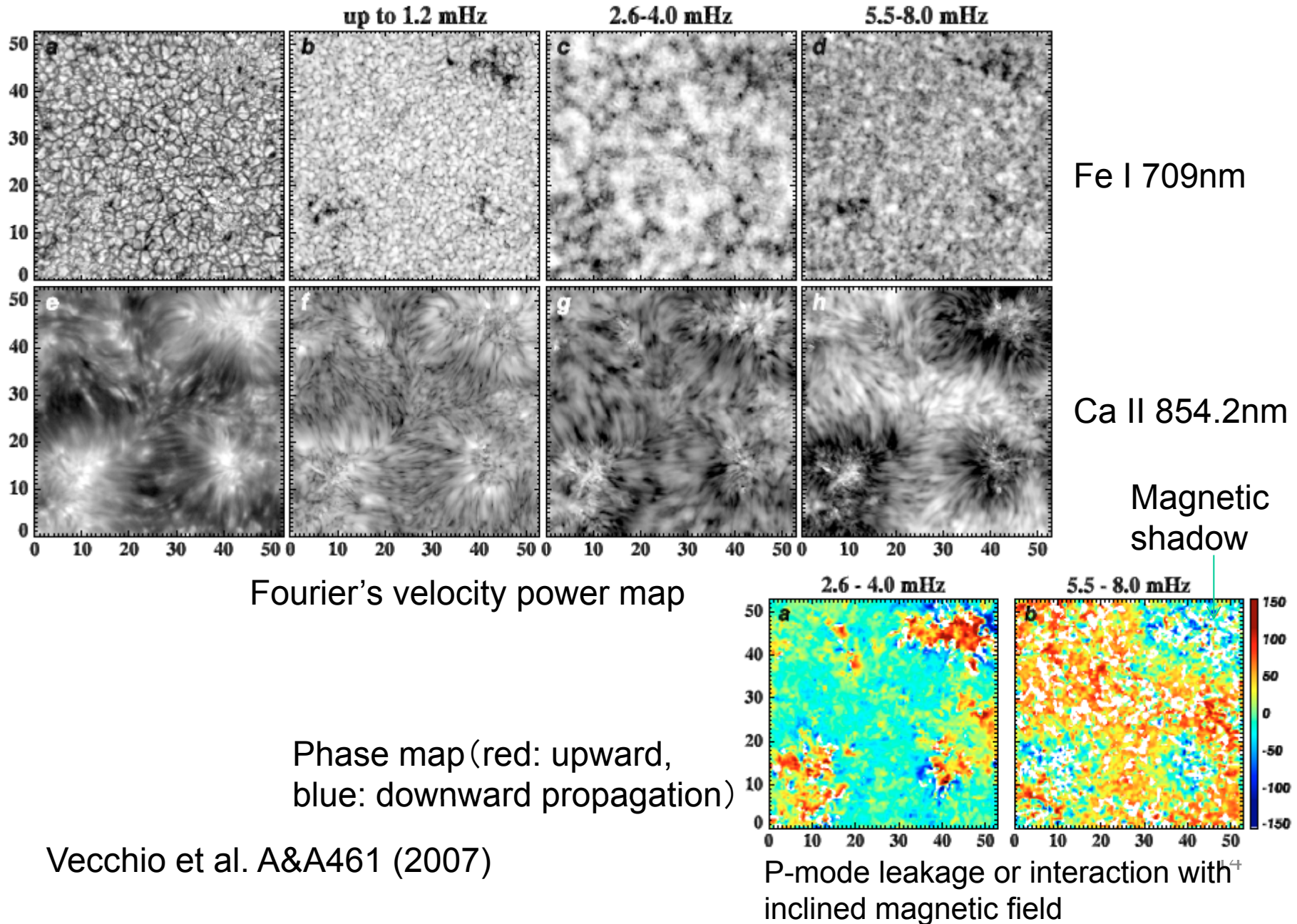
Type I: 5-min p-mode drives?

可能としても、磁場の強い活動領域の短いジェット
静穏領域の背の高いスピキュールを説明するのは難しい！



Wavelet power spectra for H α -350 m \AA and H α +350 m \AA chromospheric oscillations in fibrils showing intermittent 5-min periods (from de Pontieu and Erd'elyi (2006)).

Wave Propagation in the Chromosphere



3 min, 5 min wave propagation in Na I D

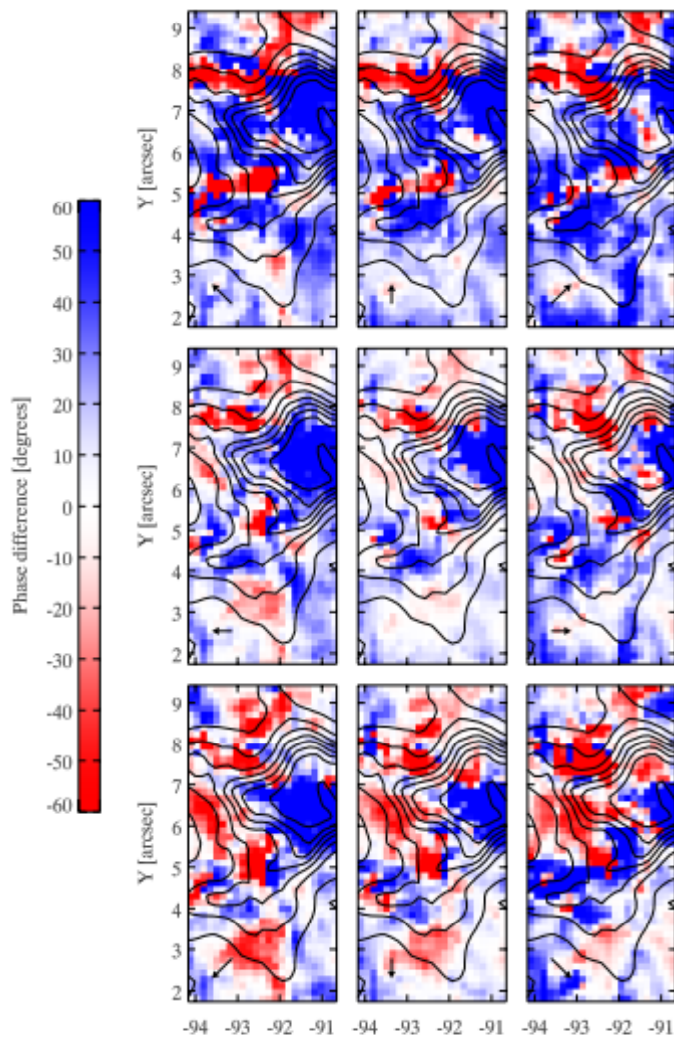


Figure 3. Phase difference between Doppler shift in Fe I and Na I D₁ at 5.6 mHz. Blue and red respectively indicate positive and negative phase difference, i.e., upward and downward propagation. Contours indicate the average Stokes V signal in Fe I at 2.5% intervals. Arrows in the bottom left corner of each panel indicate the shift between Na I D₁ and Fe I using Na I D₁ as reference. Rows are shifted in north by 3, 0, and -3 NFI pixels of $0.16'$, respectively from top to bottom. Columns are shifted east by 3, 0, and -3 NFI pixels, respectively from left to right.

li

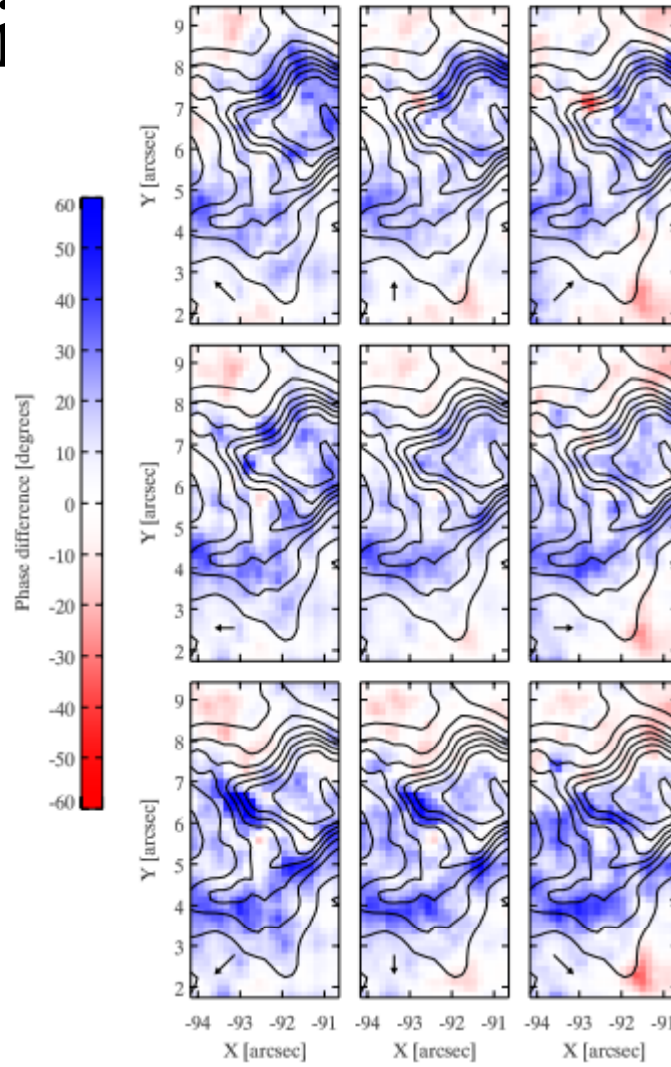


Figure 4. Phase difference between Doppler shift in Fe I and Na I D₁ at 3.3 mHz in the same format as Figure 3.

Shock wave in the Chromosphere

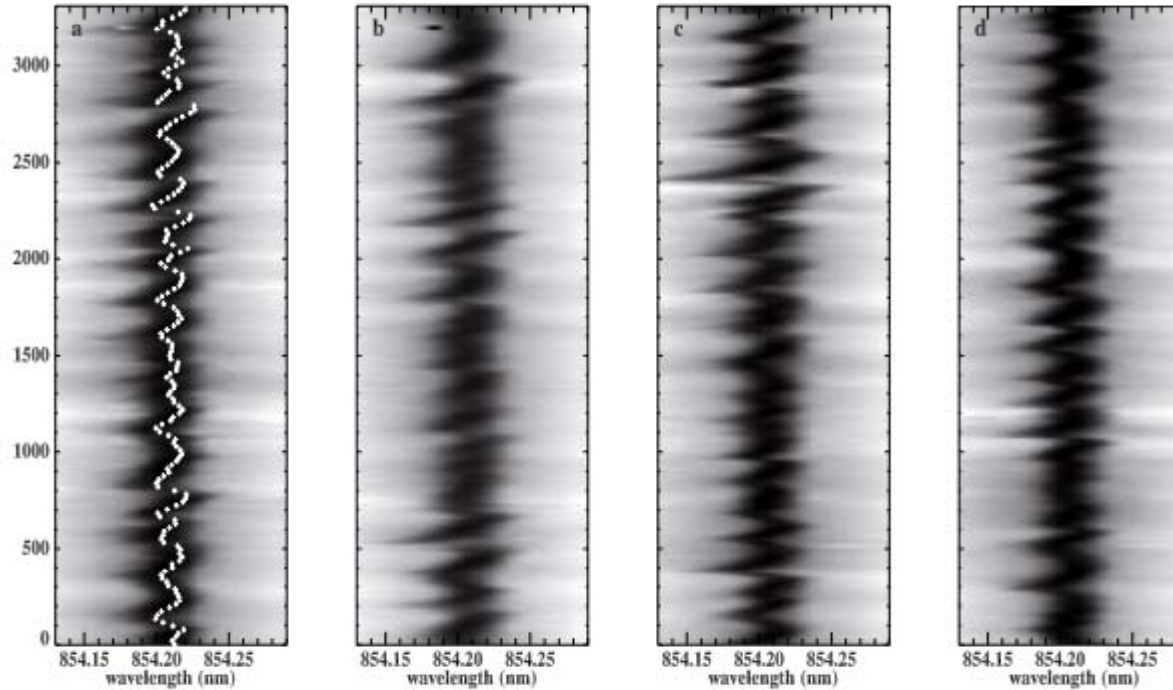
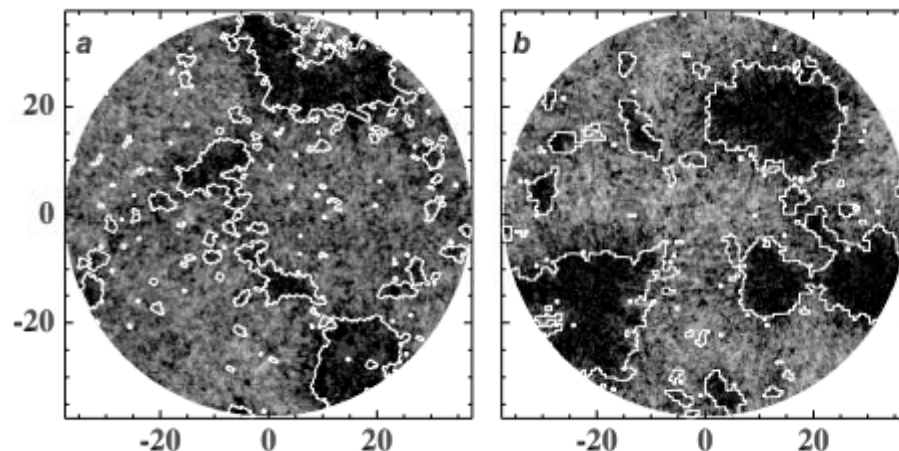


Fig. 4. Ca II 854.2 nm spectral profiles vs. time (given in s), for four positions within the internetwork. Panels **a)**, **b)** refer to data set 1; panels **c)**, **d)** to data set 2. The time axis spans the whole duration of the observations. Note the distinctive saw-tooth appearance. The thin white line in panel **a)** indicates the evolution with time of the line core Doppler shift. Maximum velocities reach $6\text{--}7 \text{ km s}^{-1}$ from average position.



Shocks avoid magnetic canopy even it is weak.

Fig. 9. Cumulative shock maps for data set 1 (panel **a)**) and 2 (panel **b)**). Overlaid is the contour of the high resolution MDI magnetic flux, averaged over the course of the IBIS observations. The contour level is set at 8 G. Compare how even minute magnetic structures within the internetwork, probably occurring only for a fraction of the observations, correspond to a decreased number of Ca II shocks. Spatial scale in arcsec.

Origin of Spicule Oscillation

Jess et al. (2012)

Observation with ROSA/DST

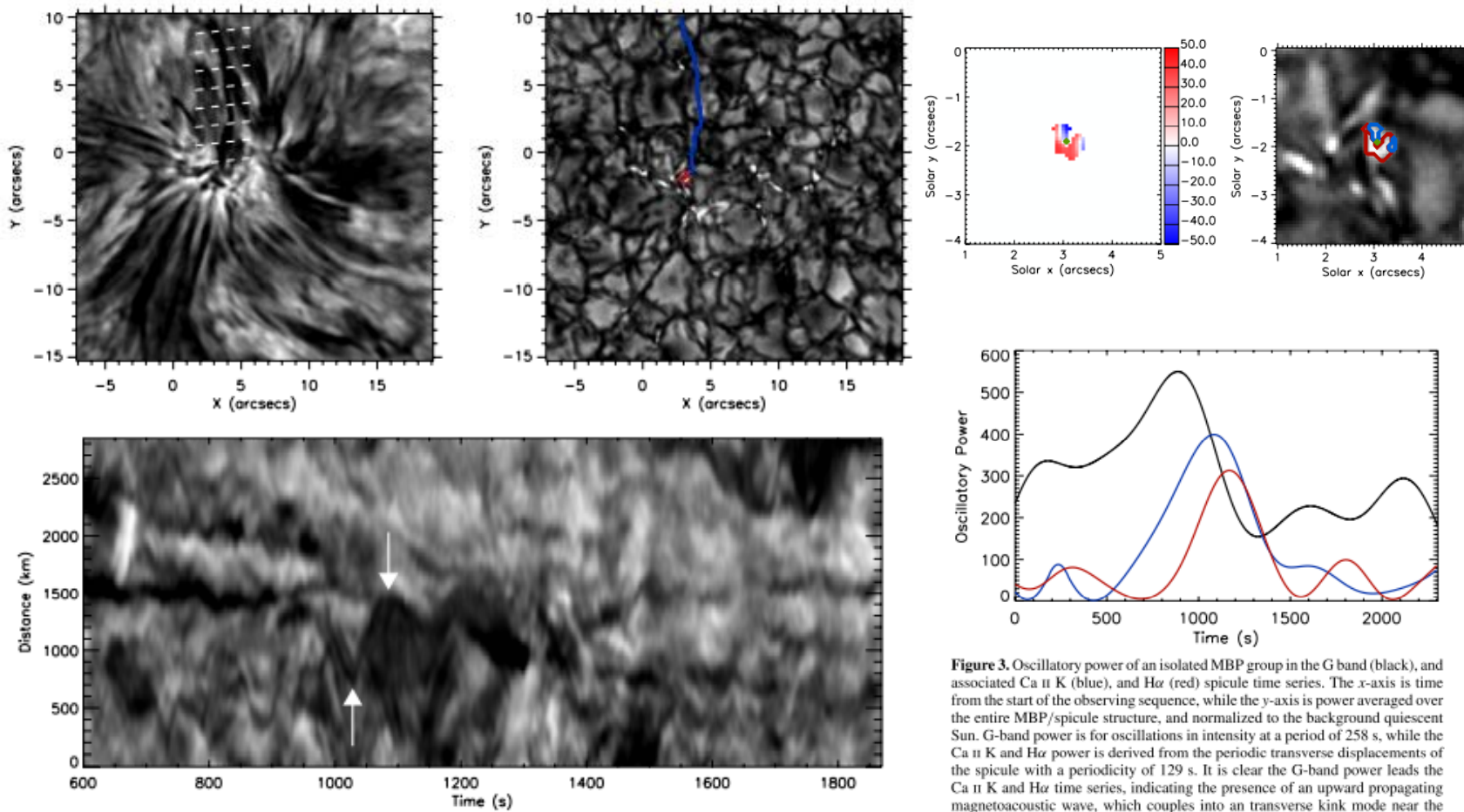
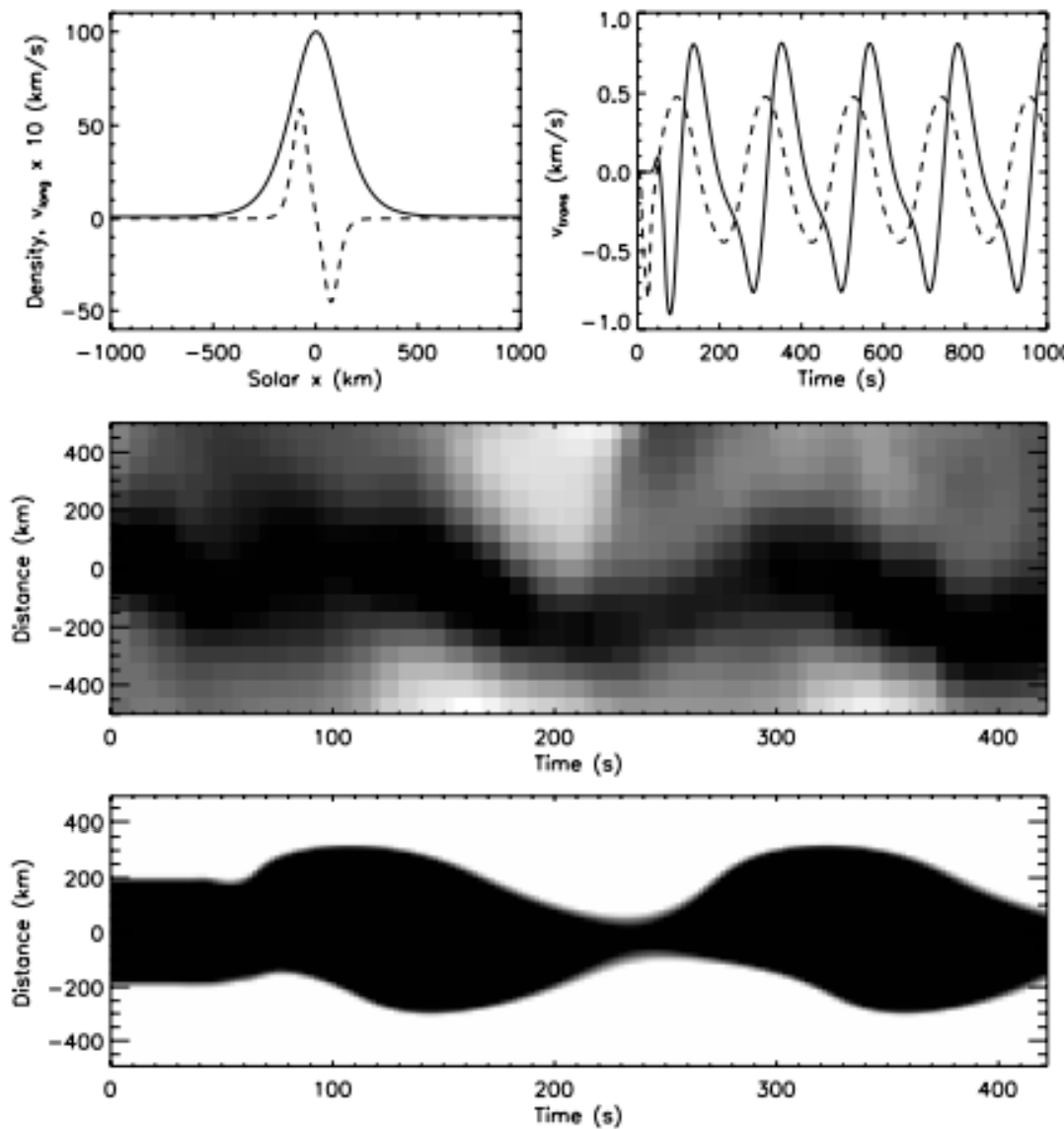


Figure 3. Oscillatory power of an isolated MBP group in the G band (black), and associated Ca II K (blue), and H α (red) spicule time series. The x-axis is time from the start of the observing sequence, while the y-axis is power averaged over the entire MBP/spicule structure, and normalized to the background quiescent Sun. G-band power is for oscillations in intensity at a period of 258 s, while the Ca II K and H α power is derived from the periodic transverse displacements of the spicule with a periodicity of 129 s. It is clear the G-band power leads the Ca II K and H α time series, indicating the presence of an upward propagating magnetoacoustic wave, which couples into an transverse kink mode near the chromospheric boundary.

Kink and Sausage mode generation by longitudinal wave



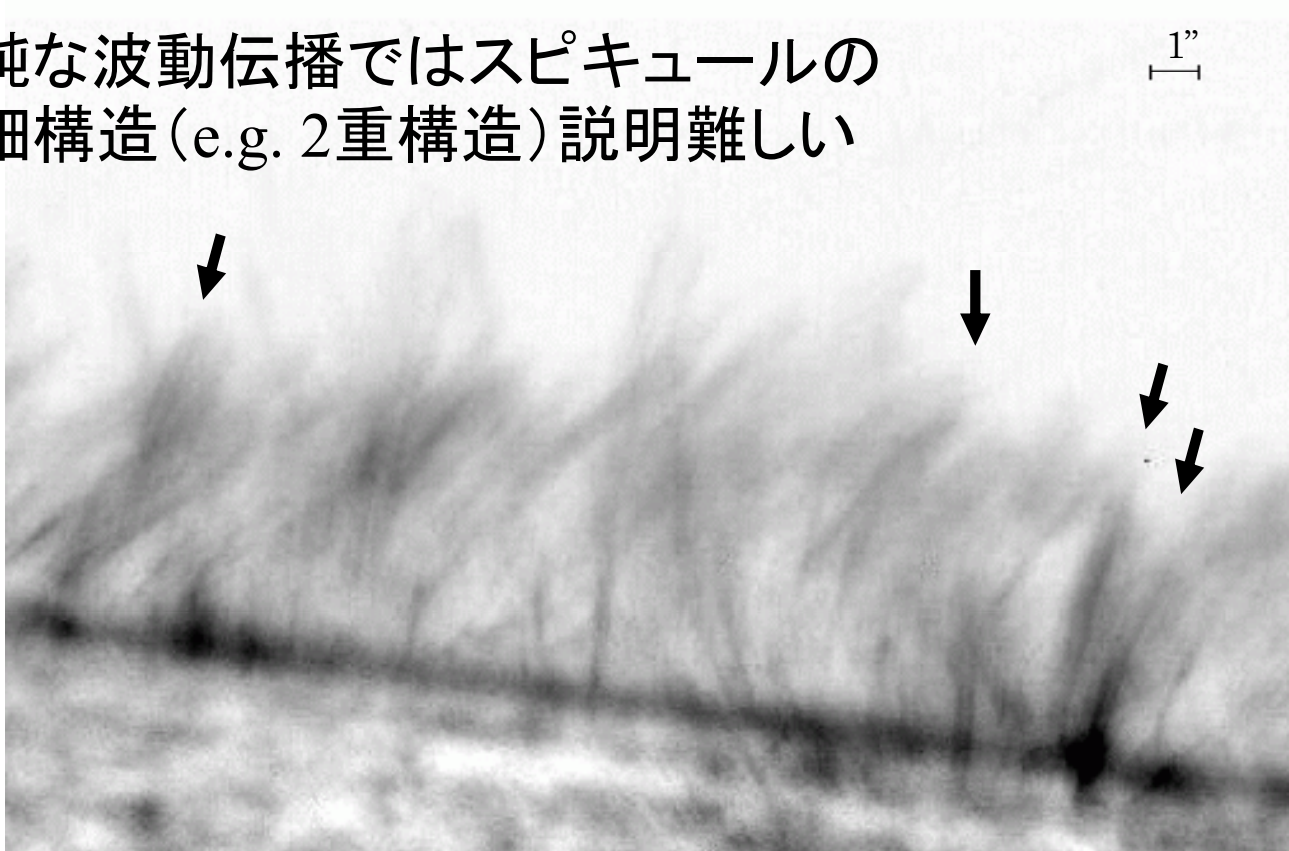
Dashed $h=500\text{ km}$
Solid $h=2000\text{ km}$

average global
energy of 660 W m^{-2} .
 $\text{Cf. } \approx 100 \text{ W m}^{-2}$
For coronal
heating

2006-11-22T06:00:27.114Z

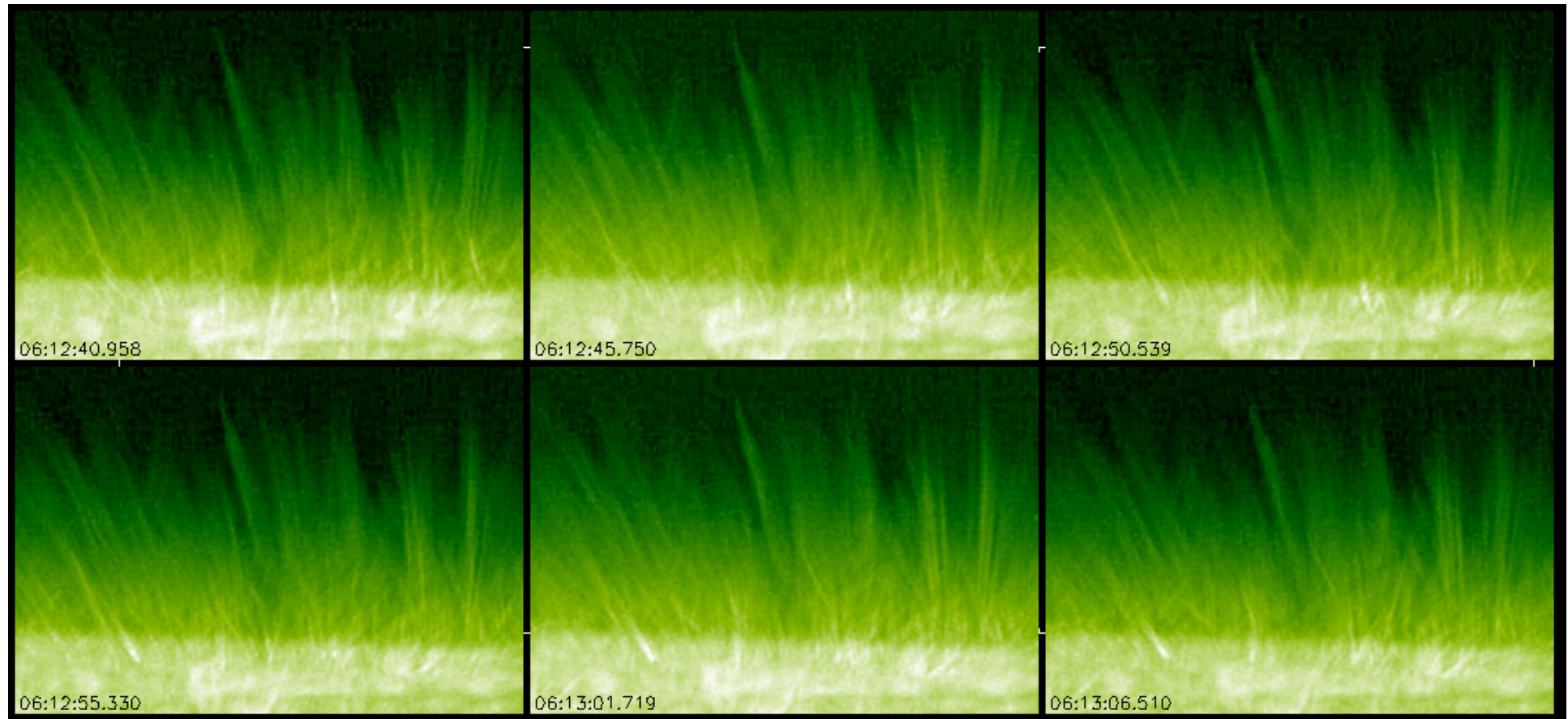
単純な波動伝播ではスピキュールの
微細構造(e.g. 2重構造)説明難しい

1"

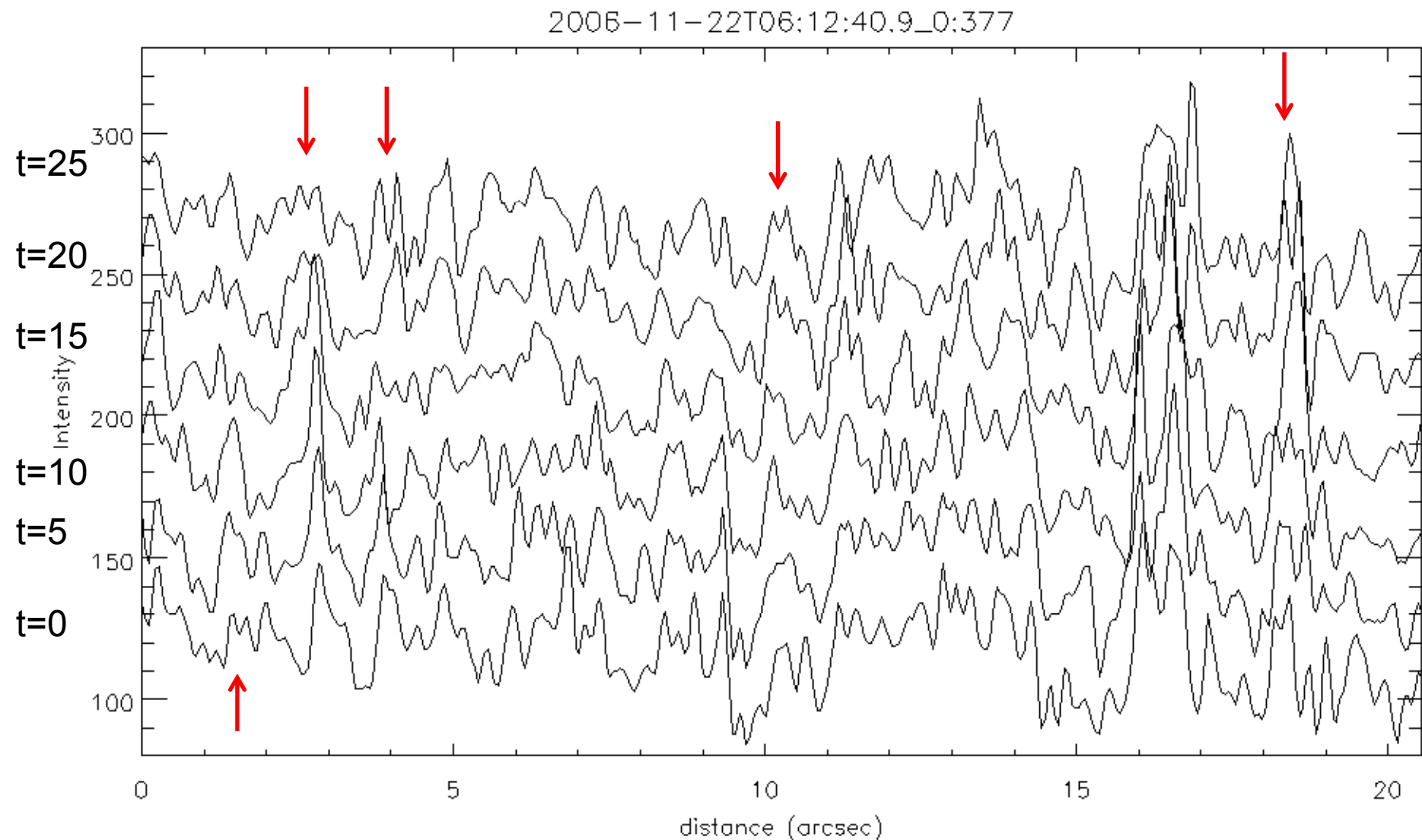


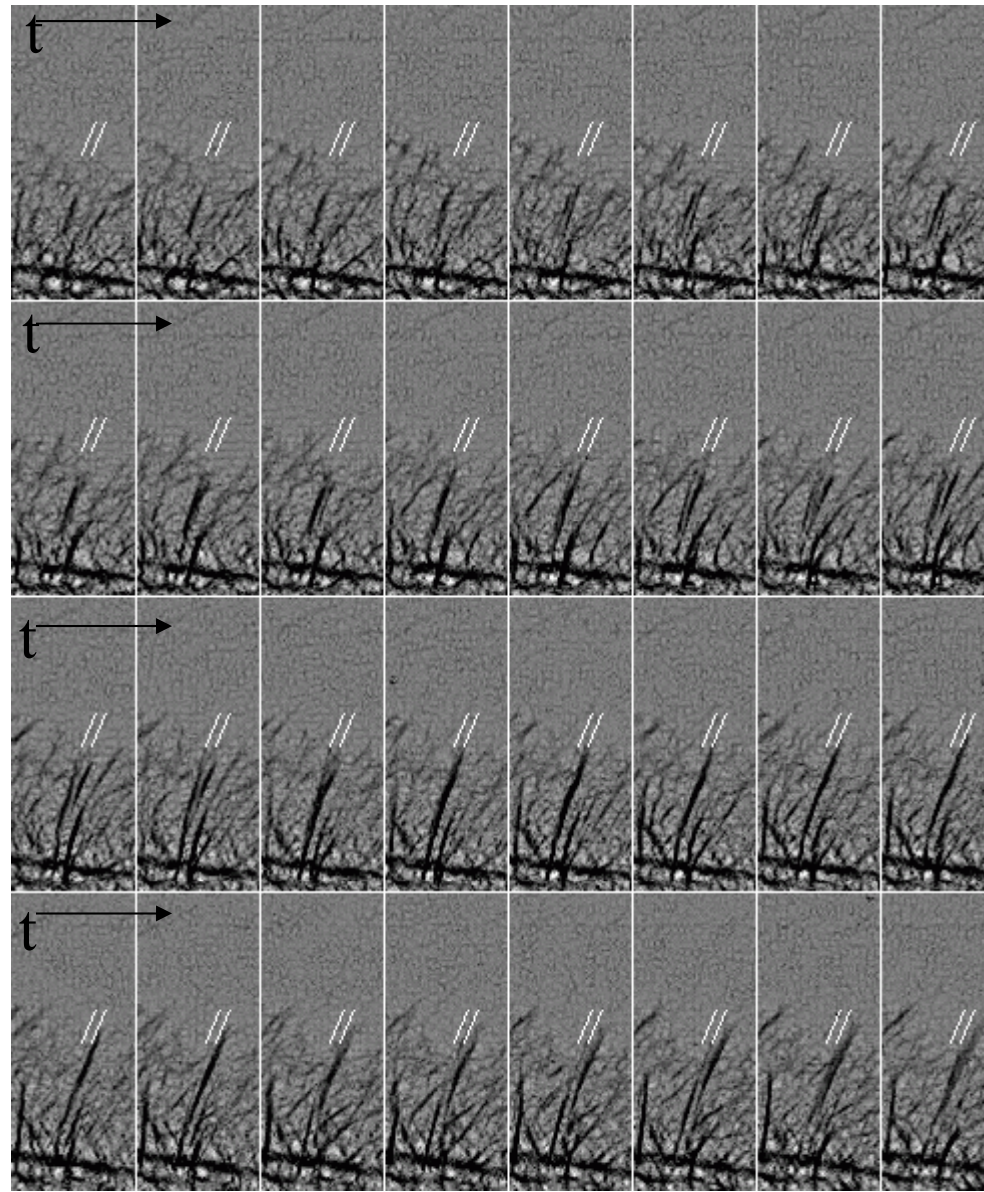
It was found that most spicules show up double thread structure during their evolution. This feature was already mentioned by Tanaka for disk mottles in high resolution H α wing observation (1974). Therefore it is likely that the spicule and disk mottles in quiet Sun have the same origin. New findings for the spicules are that the separation of the double threads change with time by the spinning as a whole body; repeating phases single and double threads.

Temporal change of double-threads



Temporal change

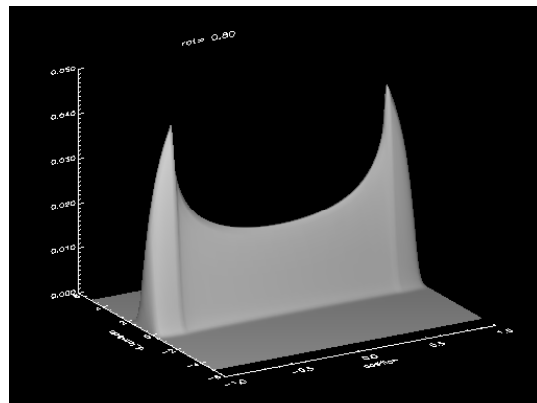
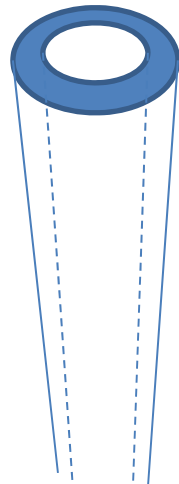
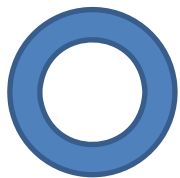




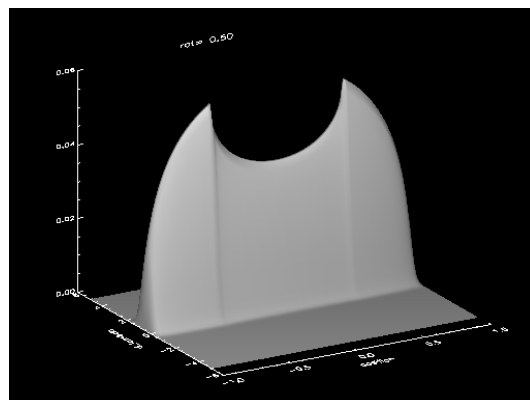
Sharpened images with a cadence of 5 sec. This series clearly show that the spicule of double threads (indicated by white lines) is spinning as a whole body (spin period: 1 - 1.5 min, $v \sim 15$ km/sec).

$$I = S(1 - \exp(-\tau))$$

$$\tau = \tau_0 \exp\left(-\left(\frac{\Delta\lambda - v\lambda_0/c}{\Delta\lambda_D}\right)^2\right)$$

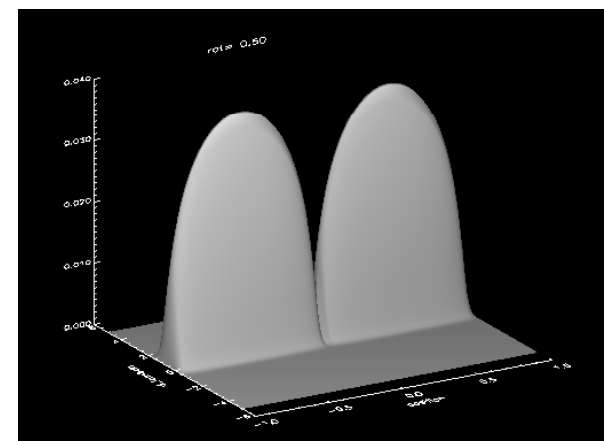
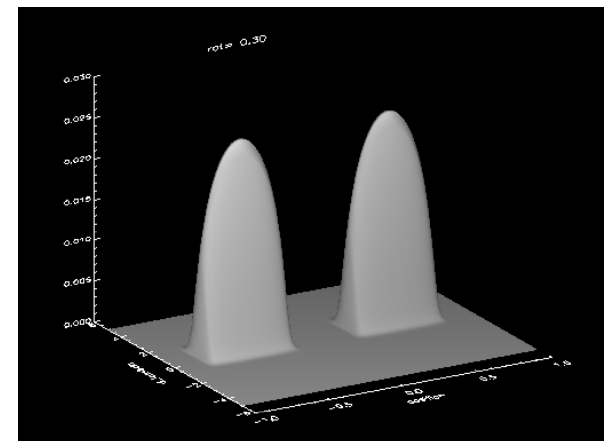
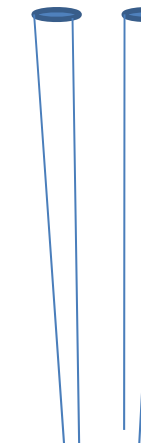
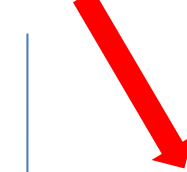


Thin shell

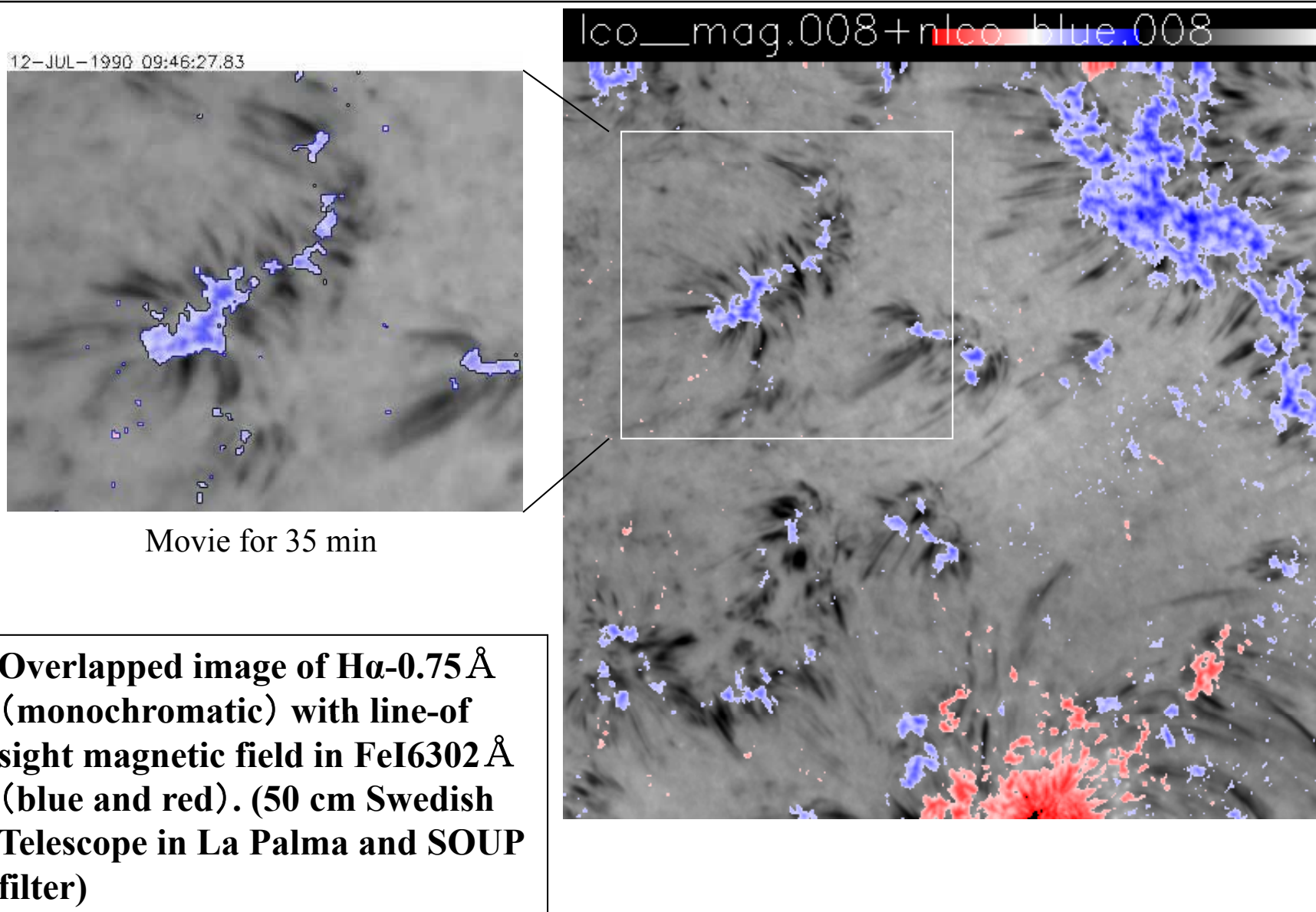


Thick shell

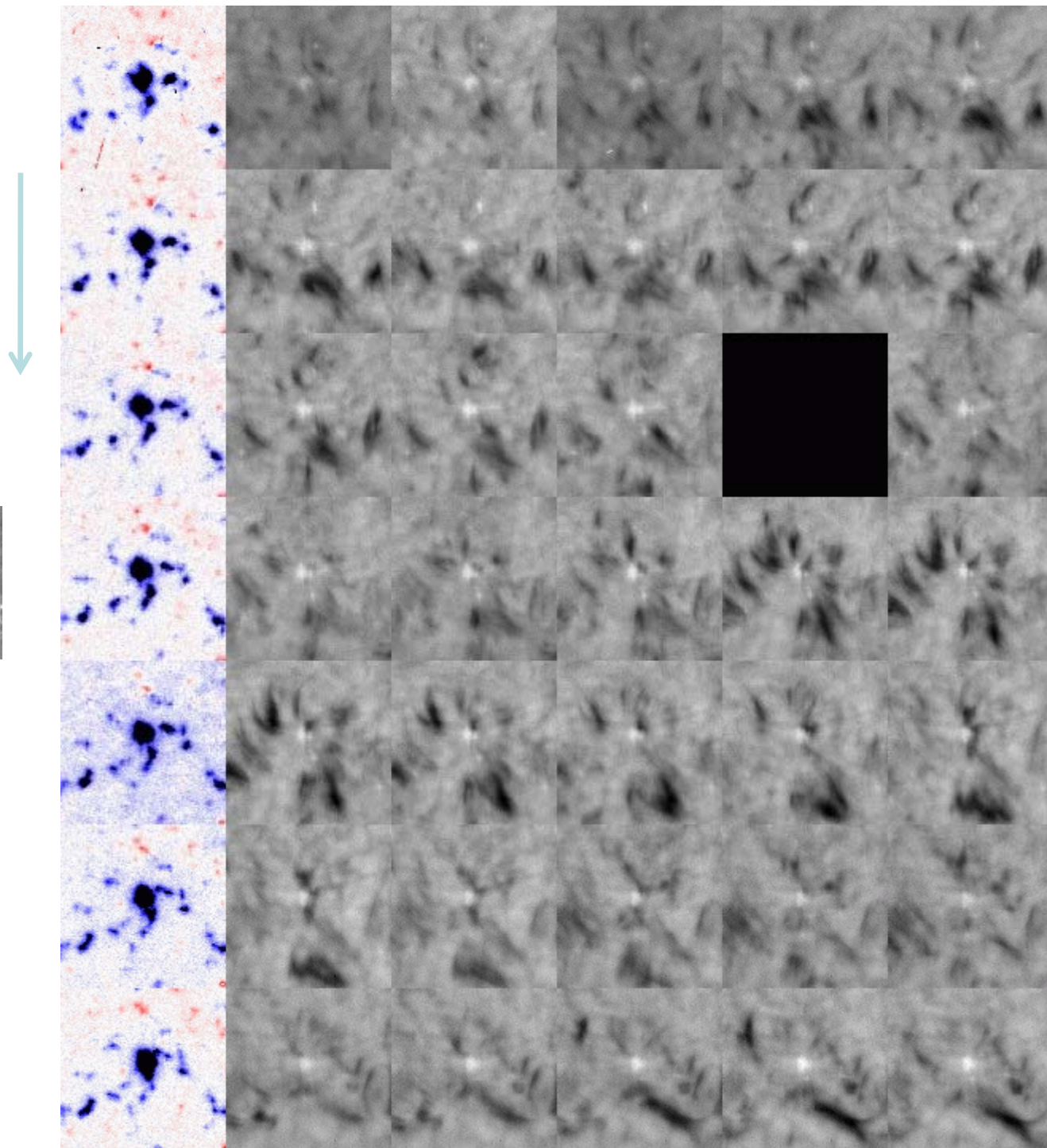
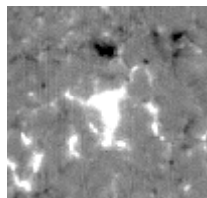
Double Thread Structure



Spicules and photospheric magnetic elements



Na D V/I
90 sec
cadence



Ha-0.6 16
sec
cadence

Vortex flows at supergranular junctions

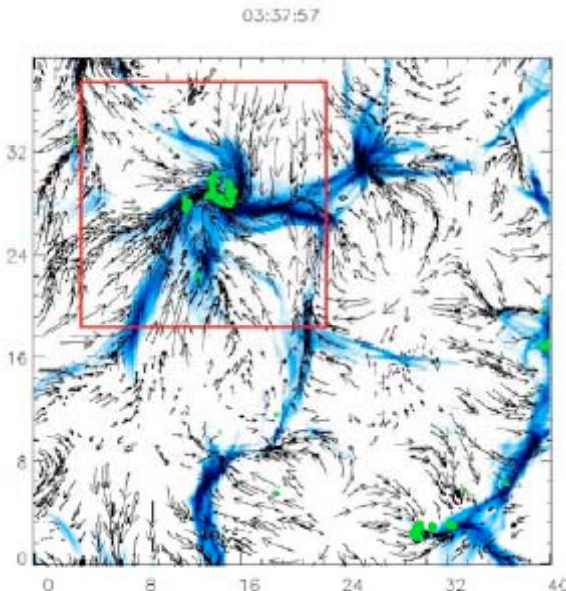


Fig. 7. Zoomed-in velocity field of Fig. 4 with a filled contour of the maximum Ca II emission. The red square indicates the patch represented in Fig. 8.

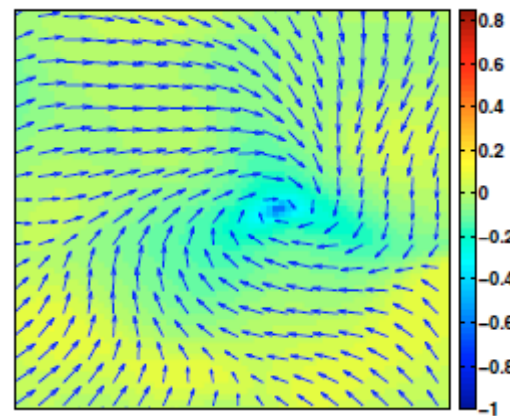
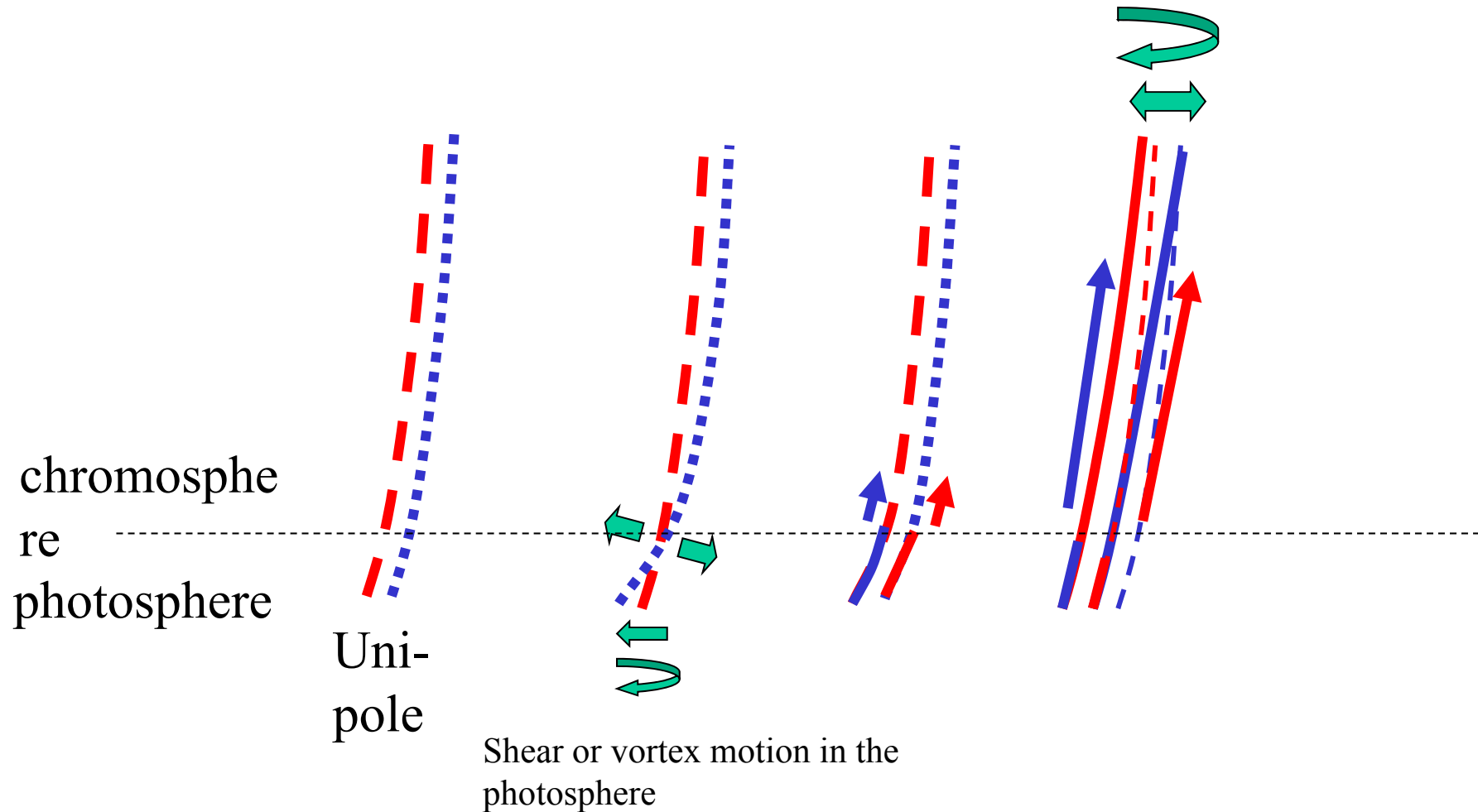


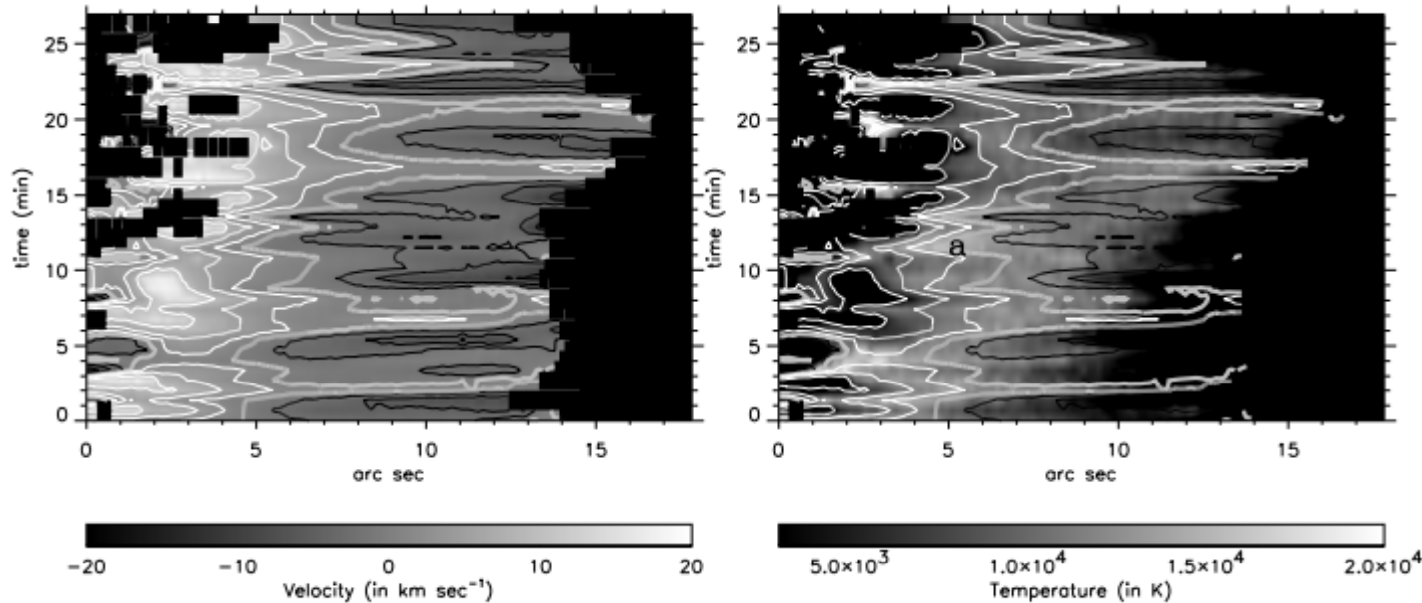
Fig. 6. Eulerian representation of the flow in the red square of Fig. 4. The colored background is the normalized vertical curl.

Attie et al. (2009, A&A493) identify long lasting vortex flow located at supergranular junctions. The first vortex flow lasts at least 1 h and is \sim 20 wide (\sim 15.5 Mm). The second vortex flow lasts more than 2 h and is \sim 27 wide (\sim 21 Mm).

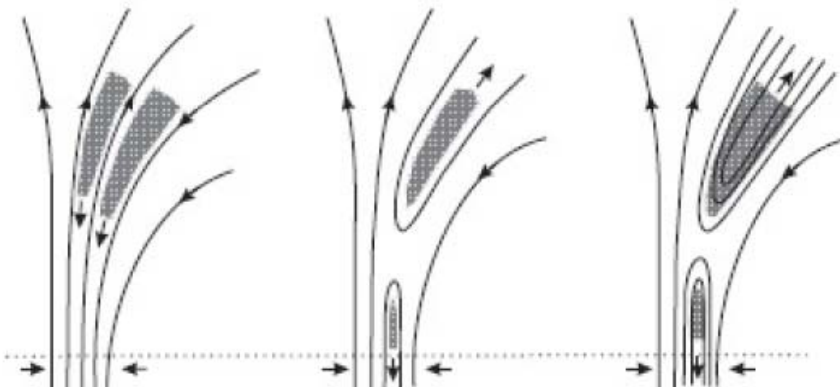


Speculative magnetic reconnection model to explain the double thread structure of spicule and following evolution (expansion thread separation, lateral motion and spinning as a whole body).

Magnetic Reconnection ?

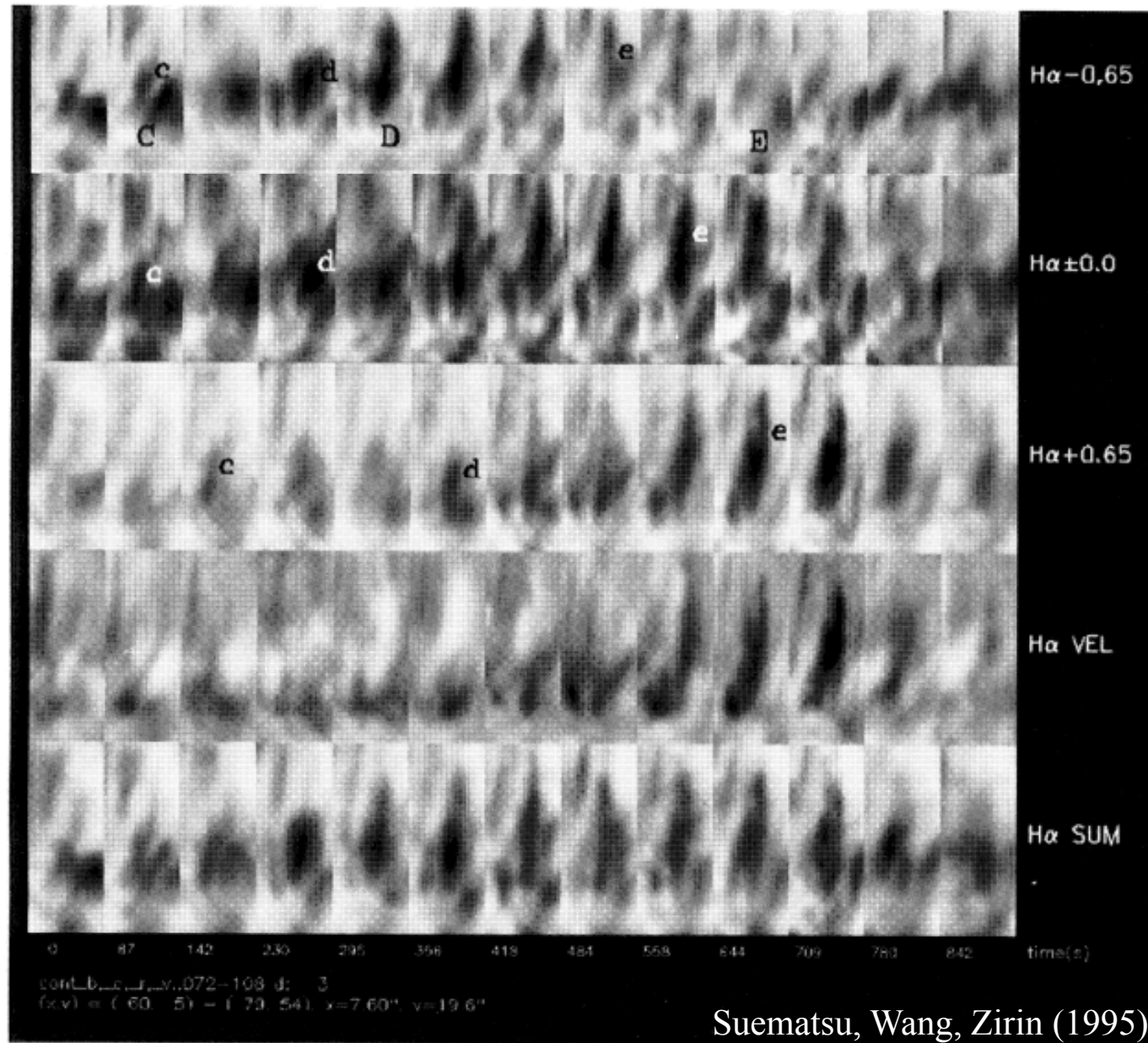


Time slice images of cloud velocity v (left) and temperature (right) along a dark mottle. On the velocity images the black contours denote upward velocities, white contours downward velocities, while the thick gray line represents the zero velocity contour (from Tziotziou et al. (2003))



A simple reconnection model explaining the observed velocity behavior in mottles, Tziotziou et al. (2003).

Motion of multi-spicules on disk



Suematsu, Wang, Zirin (1995)

FIG. 3b

Motion of spicule on disk

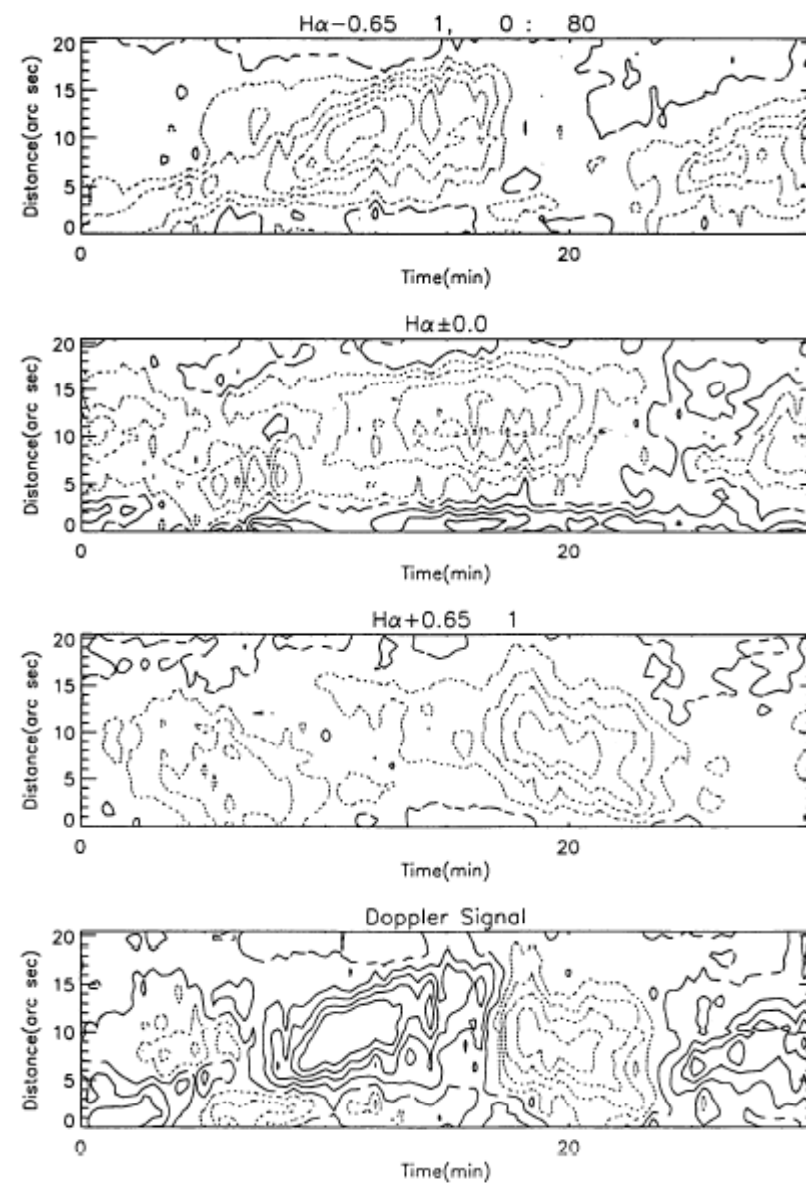
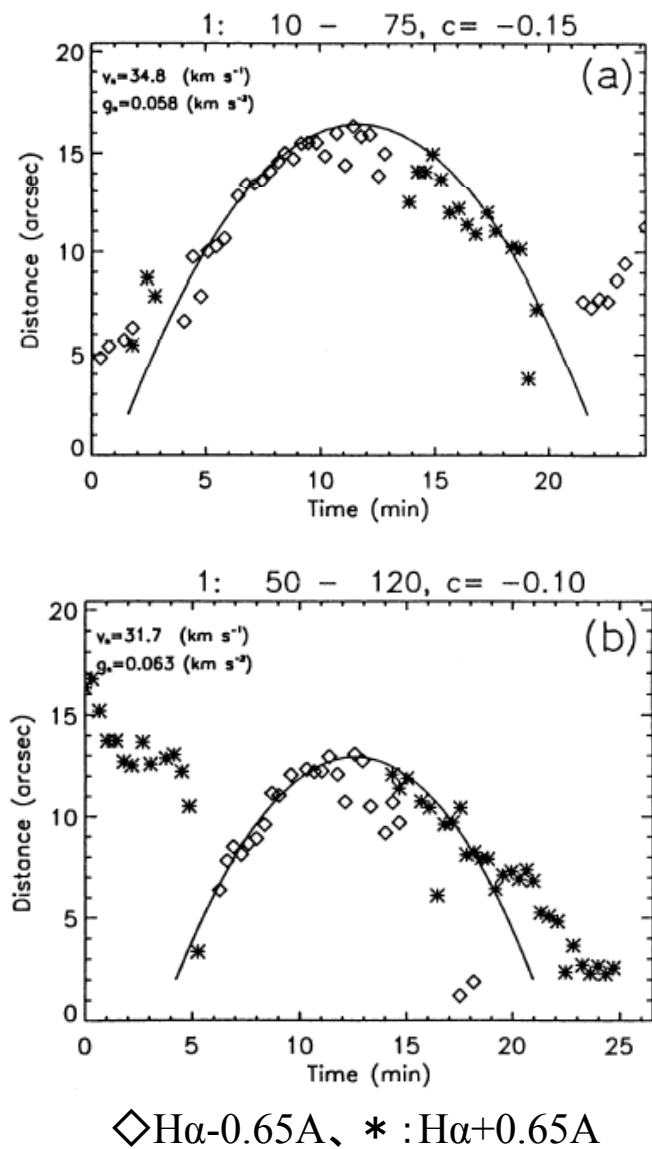


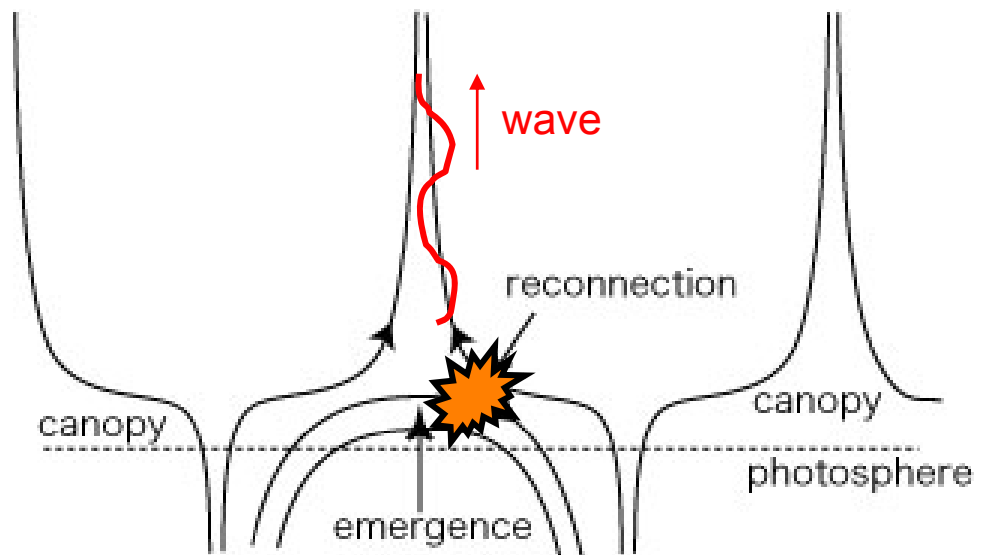
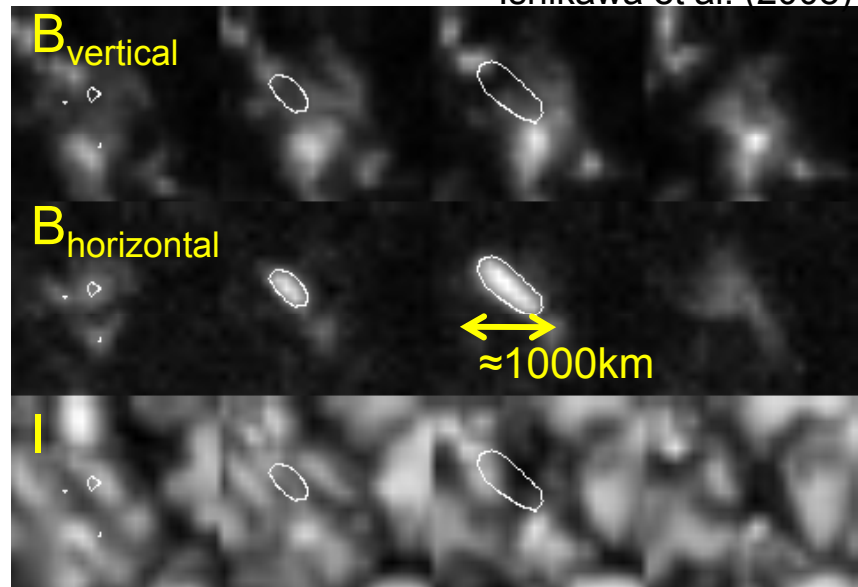
FIG. 2a

Suematsu, Wang, Zirin (1995)

Transient small-scale horizontal fields

- Ubiquitous small-scale horizontal fields found by SOT (Lites+ 2007)
- Granular-scale emerging fluxes have Poynting flux comparable to what is required to heat the corona ($\approx 10^{6-7}$ erg cm $^{-2}$ s $^{-1}$; Ishikawa & Tsuneta 2009)
- Maybe more? (Trujillo Bueno+ 2002)

Ishikawa et al. (2008)



Poynting flux can be transported by interaction with the vertical flux
(Isobe, Proctor & Weiss 2008)

Evidence of Energy Release at the Root?

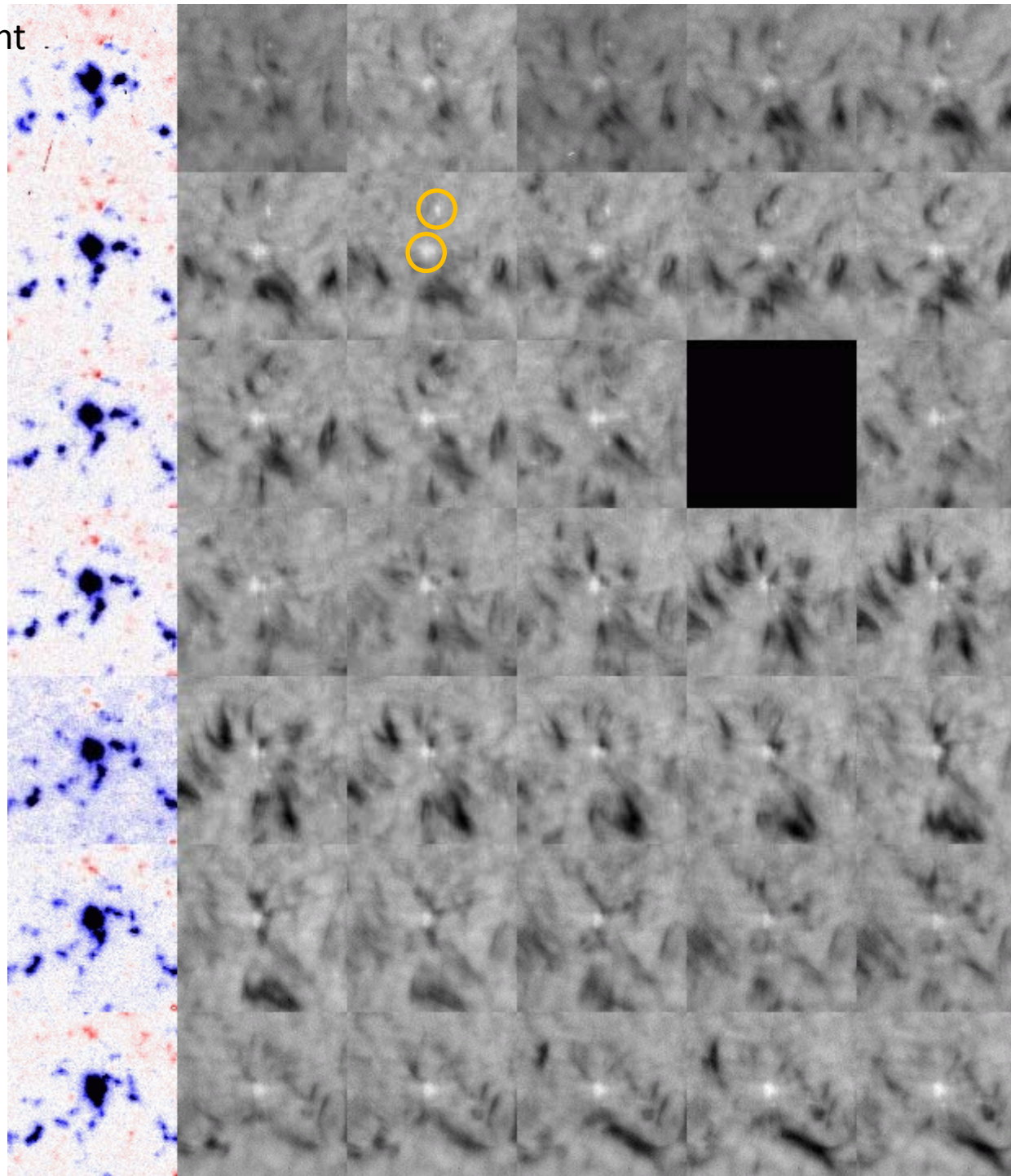
There is no doubt that the spicules are rooted at photospheric magnetic elements. So, it is quite natural to think that the network boundaries are the source of spicules, because magnetic fields concentrate there and are supposed to be responsible for the elongated structure up into the corona.

Bright points, which can be regarded as proxy of small-scale magnetic elements in the photosphere, are prominent at network boundaries in H α line-wing images under good seeing conditions (e.g. Dunn and Zirker 1973; Suematsu et al. 1995).

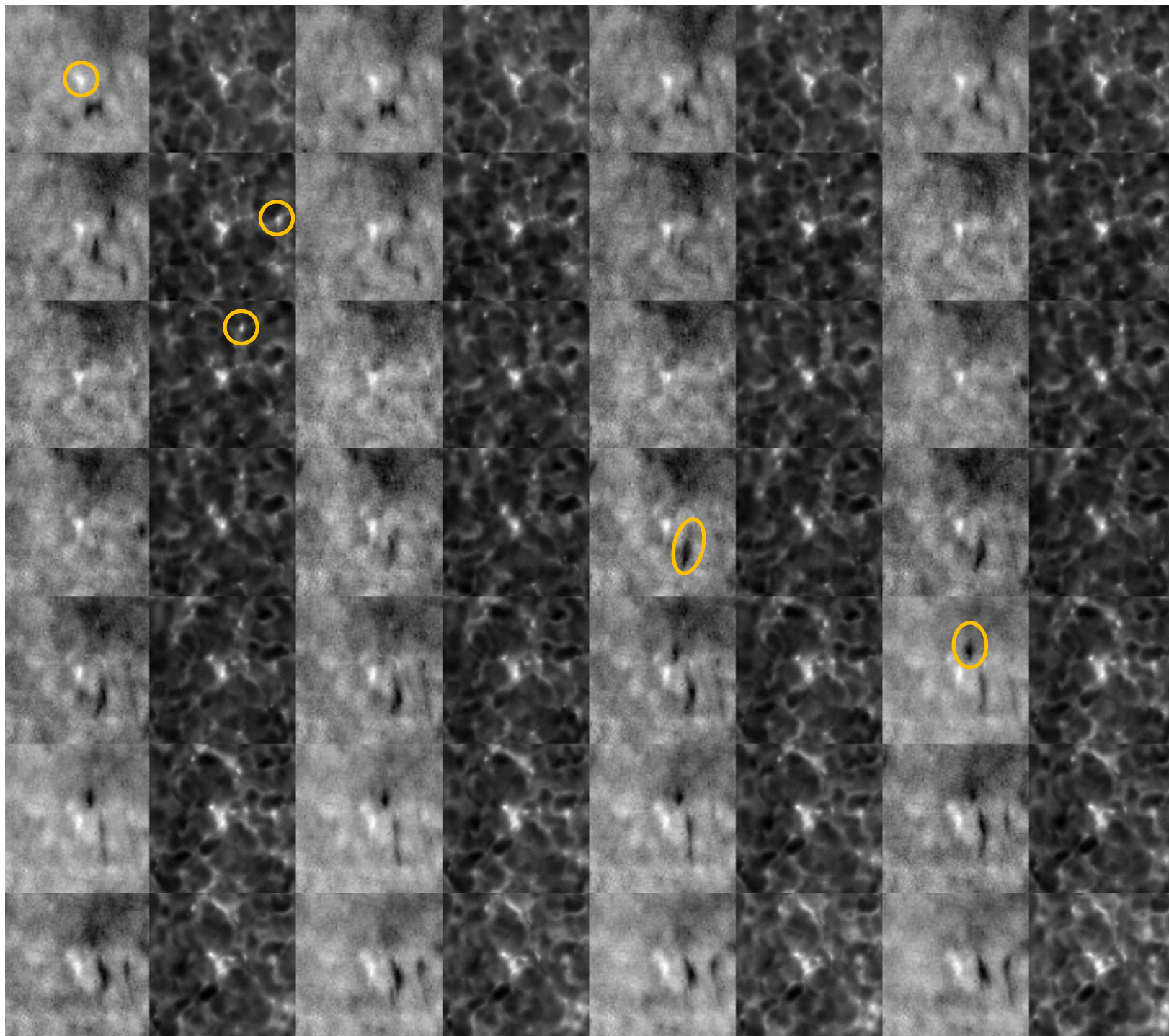
In comparing H α blue-wing with red-wing filtergrams, it is evident that bright points are very prominent at network boundaries in blue-wing while only a few appear in red-wing; spicules in red-wing are more concentrated at the network boundaries as if they blotted out the bright points or magnetic elements.

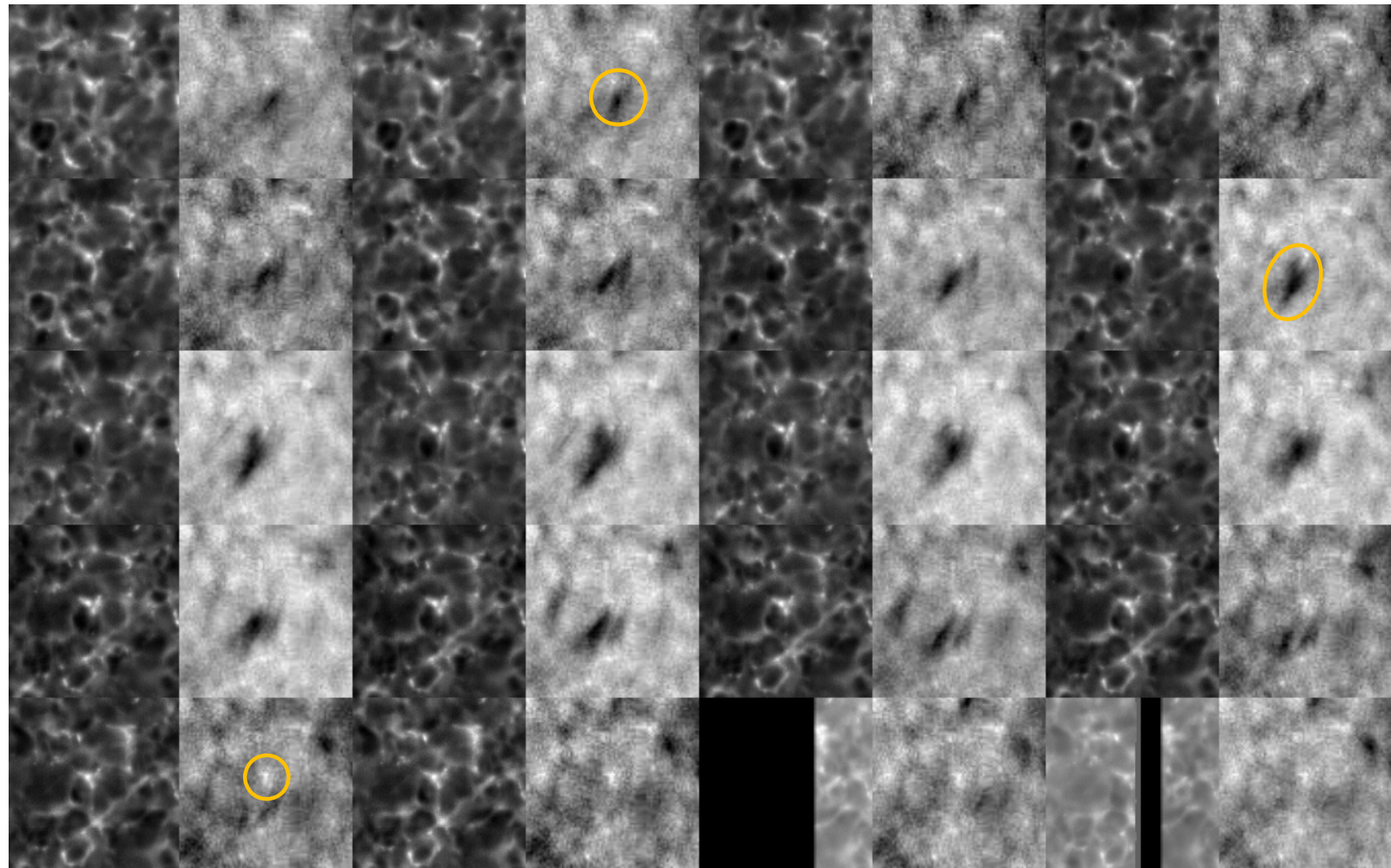
However, the relationship between the appearance of bright points and spicule formation is not clear.

Na D line-of-sight
magnetograms
90 sec cadence



→
Ha-0.6 Å
16 sec
cadence



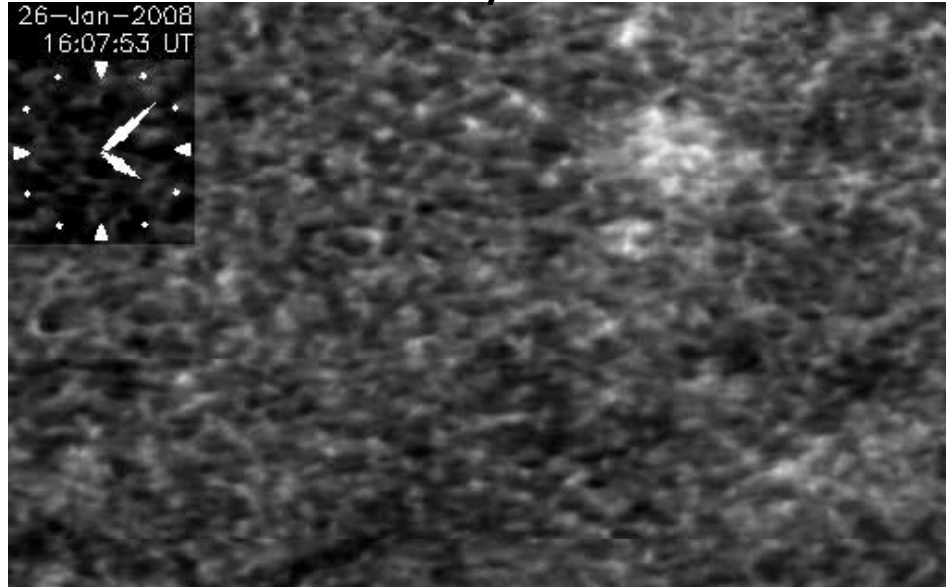


Relation of bright point appearance with spicule formation

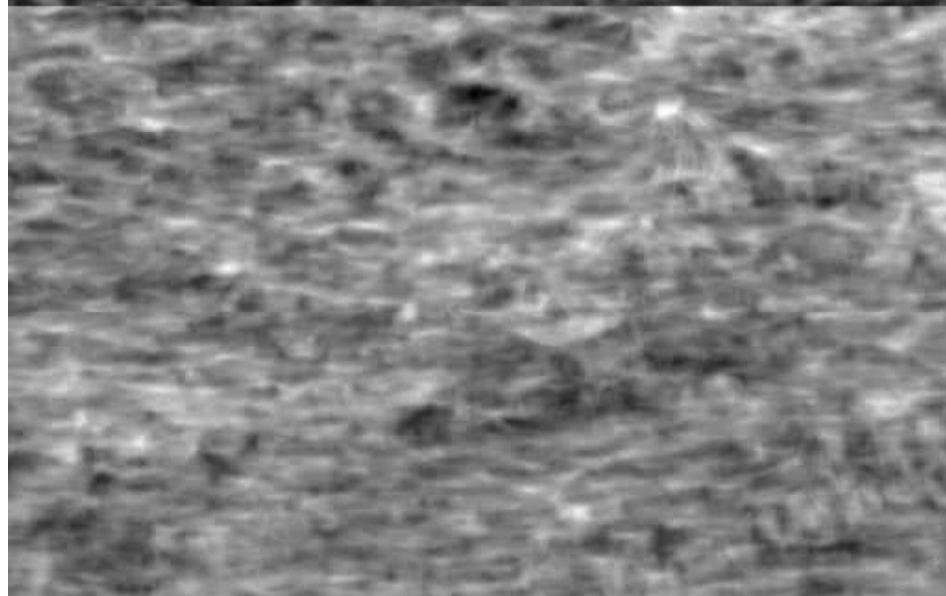
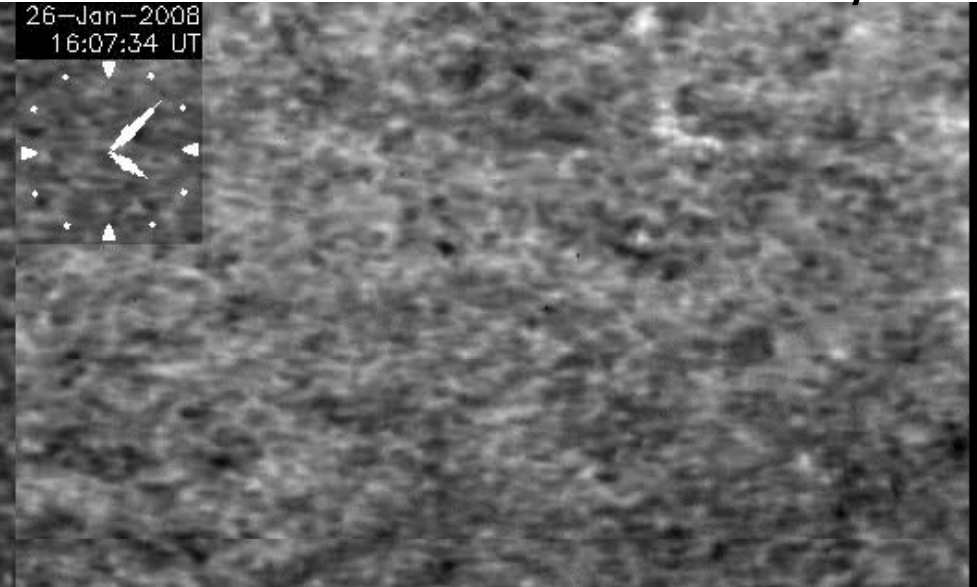
Temporal relationship	remarks	Fraction (%)
Long-lived bright points		
Bright point → spicule	It is likely that every bright points are related with spicule formation. However, we do not see any clear relation between their temporal brightness fluctuation and spicule formation.	100
Bright point → no spicule		0
Short-lived bright point		
Spicule → bright point in H α blue-wing	This class of BPs appear in extension phase or just after disappearance	50
Spicule without bright point		50

Cool(深いところ？) Spicules in Na D IVDoppler

Ca II H Intensity



Na I D Intensity



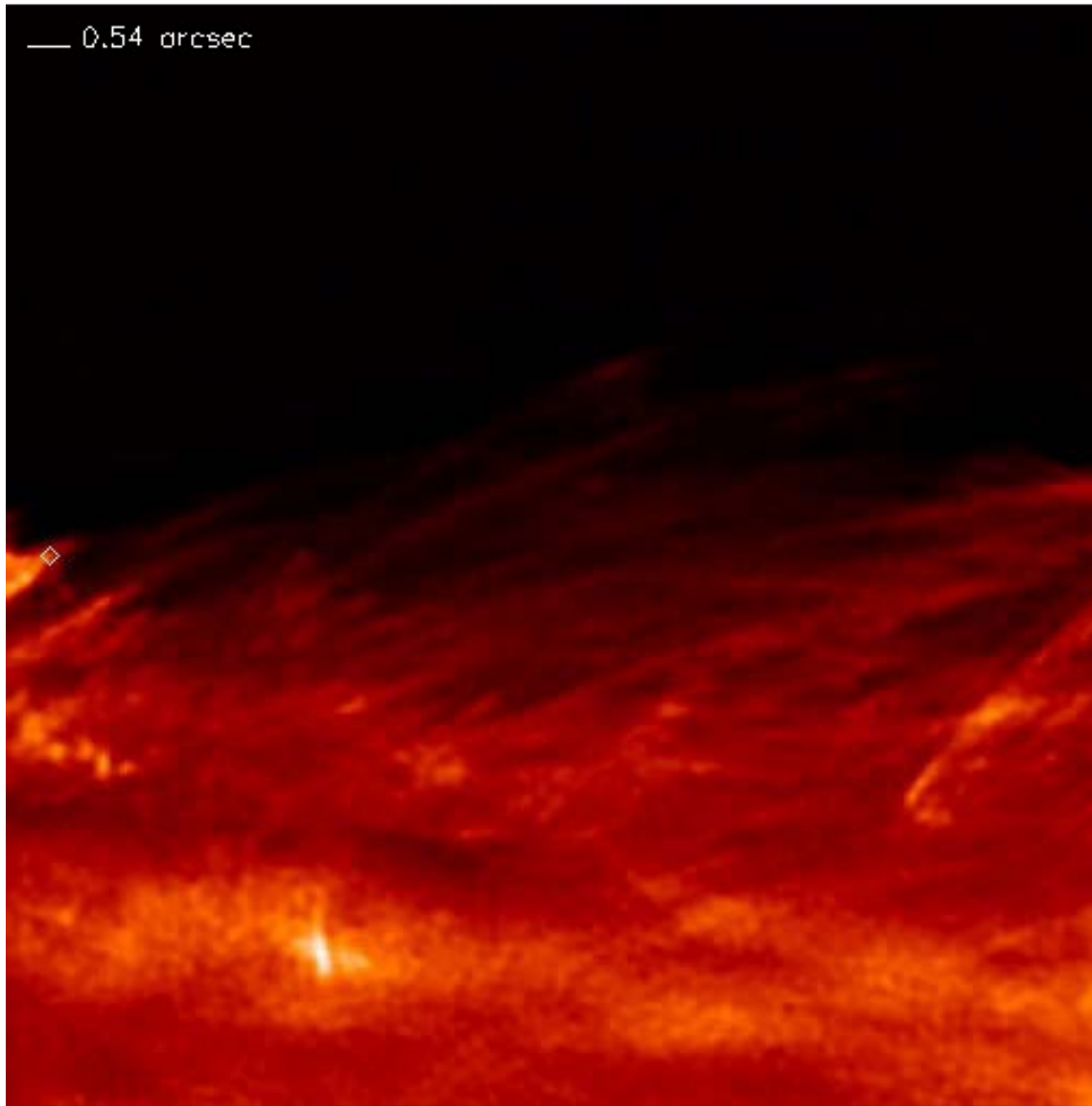
Na I D Doppler



Na I D Stokes-V

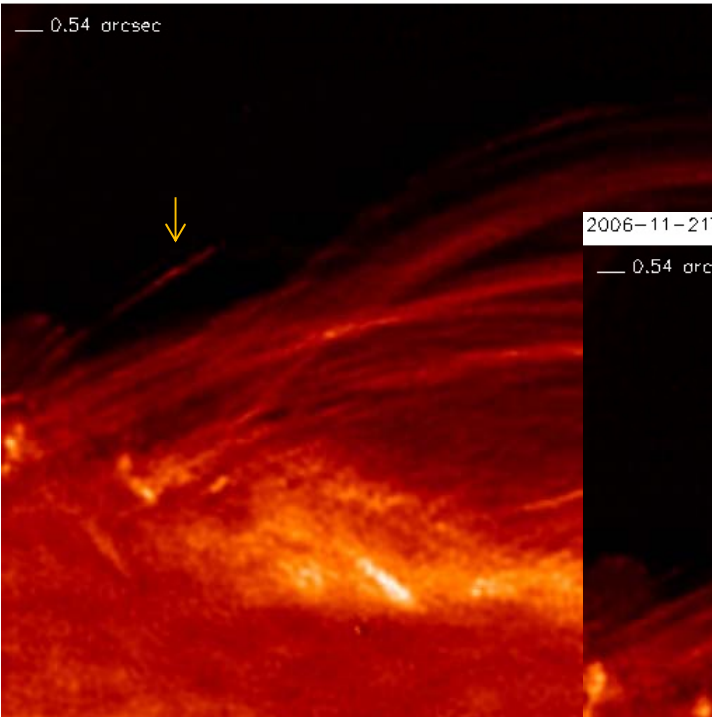
Results: Dynamics of Small-Scale Structures Revealed

2006-11-21T01:11:30.8

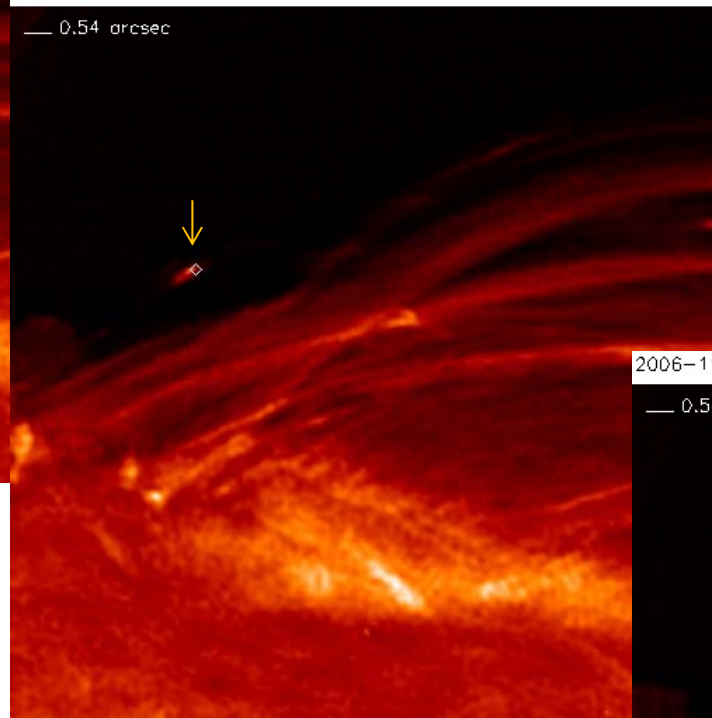


Picking peak

2006-11-21T02:52:14.0

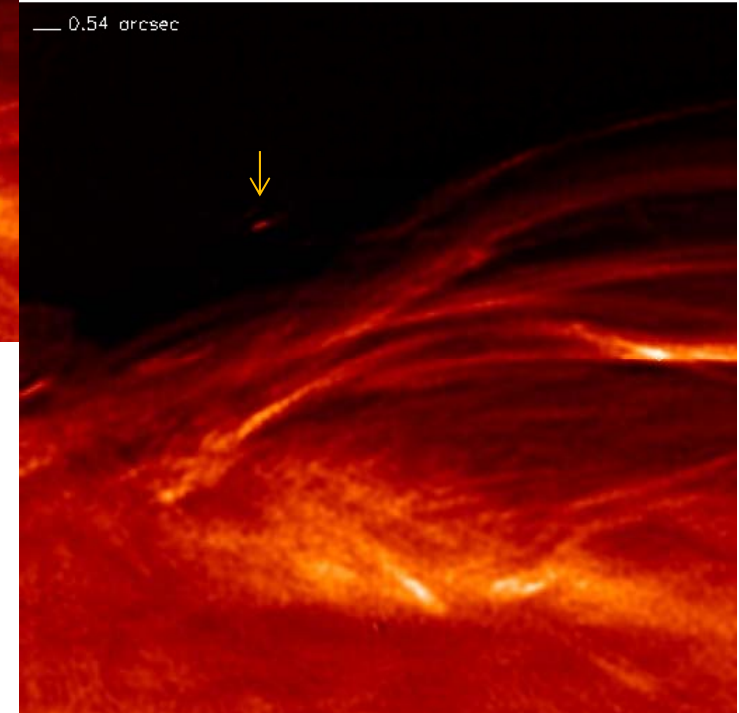


2006-11-21T02:52:22.0



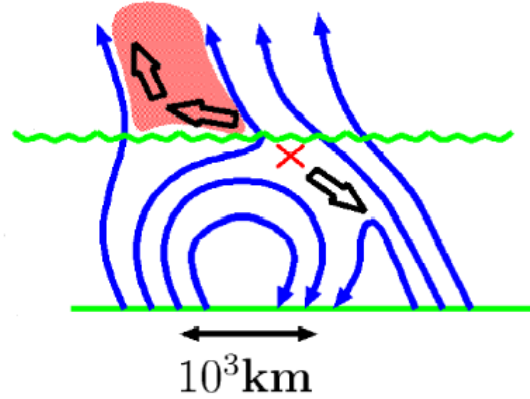
Blob formation and upward ejection

2006-11-21T02:53:01.9



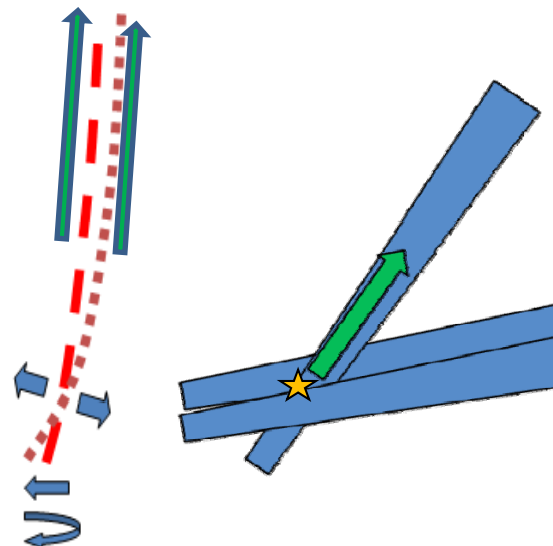
A variety of jets from current location and distribution

Most large-sized jet.
Well understood with
numerical
simulation?



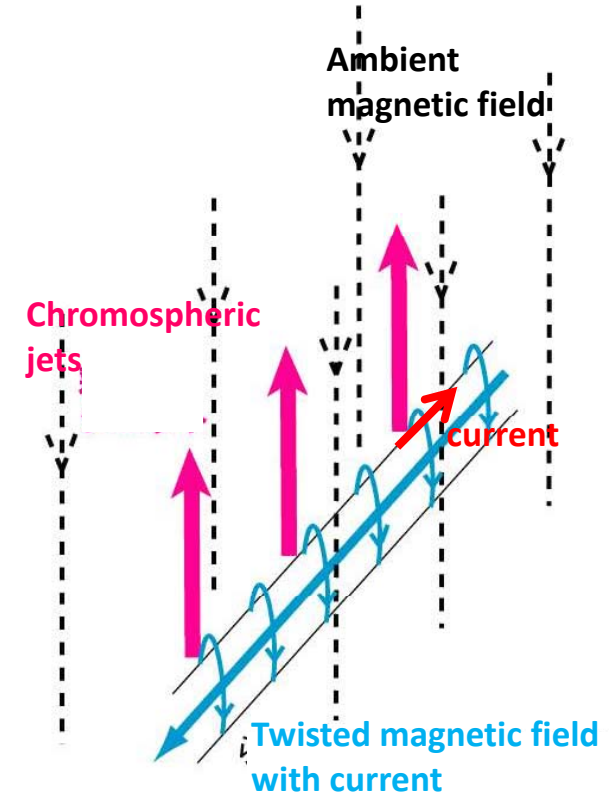
Flux emergence

Small-scale jets.
**Puzzled with large
upward velocity (100
km/s) and sudden
disappearance**



'Component' reconnection?

A group of aligned
ejections (jets)



ALMA彩層観測の期待

彩層構造の根元を見る。

磁場構造を分解

強度変化(温度変化)によるエネルギー解放、他周波数観測による
圧縮波(衝撃波)の伝播

磁場、H α ドップラー観測との同時観測

ALMAの観測諸元

FOV: >5秒角

空間分解能: <0.1秒角

時間分解能: <5秒 (0.1秒角を音波が伝播する時間以下)

周波数: 100GHz (彩層中上部)

300GHz

950GHz (T-min)

